Organometallics **1997,** *16,* 5289−5301

Clusters as Ligands. 5. Tricobalt Cluster Alkoxycarboxylates of Titanium and Zirconium Exhibiting Novel Structures and Properties

Xinjian Lei, Maoyu Shang, and Thomas P. Fehlner*

Department of Chemistry and Biochemistry, University of Notre Dame,
Notre Dame, Indiana 46556

Received September 23, 1997[⊗]

The protonolysis of group 4 M(IV)(OR)$_4$, M = Ti, Zr, organic alkyl- or aryloxides with the cluster acid $(CO)_9Co_3(\mu_3\text{-}CCO_2H)$ leads to a series of novel tricobalt cluster M(IV) alkoxy- or aryloxycarboxylates, most of which contain bridging oxo ligands. The compounds, which are isolated in good yield as crystalline substances and characterized spectroscopically as well as crystallographically, are $Zr_2(\mu\text{-}OCH(CH_3)_2)_2(OCH(CH_3)_2)_2\{\mu\text{-}(CO)_9Co_3(\mu_3\text{-}CCO_2)\}_2\{(CO)_9\text{-}Co_3(\mu_3\text{-}CCO_2)\}_2$, **1**; $Ti_4(\mu_3\text{-}O)_4(OR)_4\{\mu\text{-}(CO)_9Co_3(\mu_3\text{-}CCO_2)\}_4$, **2** (R = $CH(CH_3)_2$, **2a**; $(CH_2)_3CH_3$, **2b**; C_6H_5, **2c**; 2,6-$(CH_3)_2$-C_6H_3, **2d**); $Ti_6(\mu_3\text{-}O)_4(\mu\text{-}OCH_2CH_3)_4(OCH_2CH_3)_8\{\mu\text{-}(CO)_9Co_3(\mu_3\text{-}CCO_2)\}_4$, **3**; and $[Ti_6(\mu_3\text{-}O)_2(\mu\text{-}O)_2(\mu\text{-}OCH(CH_3)_2)_2(OCH(CH_3)_2)_2(1,2\text{-}O_2C_6H_4)_4\{\mu\text{-}(CO)_9Co_3(\mu_3\text{-}CCO_2)\}_4]$, **4**. Further, the mixed-metal derivatives $[Ti_2Co_2\{(OCH_2)_3CCH_3\}_2(OCH(CH_3)_2)_2\{\mu\text{-}(CO)_9Co_3(\mu_3\text{-}CCO_2)\}_4]$, **5**, and $[\{Co_3Ti(OCH_3)_6(HOCH_3)(THF)\{\mu\text{-}(CO)_9Co_3(\mu_3\text{-}CCO_2)\}_3\}_2(O_2\text{-}CCO_2)]\cdot 2HOCH_3\cdot 2THF$, **6**, in which the Co(II) ions are derived from *in situ* tricobalt cluster degradation, are characterized in similar fashion. Some of the distinguishing features of an inorganic cluster as a ligand substituent are revealed by a comparison of the observed chemistry with that known for reactions of organic acids with M(IV)(OR)$_4$.

Introduction

By logical variation of steric and electronic factors, organic substituents can be used to modify the coordination chemistry of numerous ligand types. Indeed, the development of functionalized organic compounds constitutes the dominant approach to the adjustment and control of ligand properties. Since the time of Werner, inorganic moieties have been occasionally used as substituents and often generate dramatically different effects from those of organic moieties.[1−7]

We are interested in the effects of transition metal cluster substituents on metal carboxylate coordination chemistry which utilizes the $[(CO)_9Co_3(\mu_3\text{-}CCO_2)]^-$ ligand derived *in situ* from the free acid.[8−10] Use of the acid form is necessary as the tricobalt carbonyl cluster rapidly degrades under basic conditions. In terms of synthetic approaches, the protonolysis of metal alkyls and the exchange of organic metal carboxylates have led to a number of interesting compounds.[11,12] In these investigations, we have found that cluster degradation competes with the simple coordination chemistry and, when the coordination reactions are sluggish, some unexpected and unusual compounds are found as products.[13] Although this degradation chemistry measurably perturbs the coordination chemistry, it still leads to the isolation of single cluster assemblies in good yields.

In both types of products, the cluster substituent has a nontrivial effect on the chemistry and properties. For example, new metal carboxylate structures are captured,[14,15] large perturbations in the absorption properties are observed in certain instances,[16] and qualitative changes in the redox behavior is also found.[17] In addition, these cluster assemblies have been found to be precursors for novel catalytic materials[11,18] with unusual activities and selectivities for demanding hydrogenations.[19] Chemistry related to this cluster has appeared,[20,21] and most recently, others have reported

---

[⊗] Abstract published in *Advance ACS Abstracts,* November 15, 1997.

(1) Seyferth, D.; Kugita, T.; Rheingold, A. L.; Yap, G. P. A. *Organometallics* **1995**, *14*, 5362.

(2) Yeung, L. K.; Kim, J.-E.; Chung, Y. K.; Rieger, P. H.; Sweigart, D. A. *Organometallics* **1996**, *15*, 3891.

(3) Yang, X.; Knobler, C. B.; Hawthorne, M. F. *J. Am. Chem. Soc.* **1993**, *115*, 4904.

(4) Morgenstern, D. A.; Ferrence, G. M.; Washington, J.; Henderson, J. I.; Rosenhein, L.; Heise, J. D.; Fanwick, P. E.; Kubiak, C. P. *J. Am. Chem. Soc.* **1996**, *118*, 2198.

(5) Jordan, M. R.; White, P. S.; Schauer, C. K.; Mosley, M. A., III *J. Am. Chem. Soc.* **1995**, *117*, 5403.

(6) Hao, L.; Vittal, J. J.; Puddephatt, R. J. *Inorg. Chem.* **1996**, *35*, 269.

(7) Achar, S.; Vittal, J. J.; Puddephatt, R. J. *Organometallics* **1996**, *15*, 43.

(8) Penfold, B. R.; Robinson, B. H. *Acc. Chem. Res.* **1973**, *6*, 73.

(9) Seyferth, D. *Adv. Organomet. Chem.* **1976**, *14*, 97.

(10) Lindsay, P. N.; Peake, B. M.; Robinson, B. H.; Simpson, J. *Organometallics* **1984**, *3*, 413.

(11) Bañares, M. A.; Dauphin, L.; Lei, X.; Cen, W.; Shang, M.; Wolf, E. E.; Fehlner, T. P. *Chem. Mater.* **1995**, *7*, 553.

(12) Cen, W.; Haller, K. J.; Fehlner, T. P. *Inorg. Chem.* **1991**, *30*, 3120.

(13) Cen, W.; Haller, K. J.; Fehlner, T. P. *Organometallics* **1992**, *11*, 3499.

(14) Lei, X.; Shang, M.; Patil, A.; Wolf, E. E.; Fehlner, T. P. *Inorg. Chem.* **1996**, *35*, 3217.

(15) Lei, X.; Shang, M.; Fehlner, T. P.; Werner, R.; Haase, W.; Hautot, D.; Long, G. J. *J. Organomet. Chem.* **1997**, *541*, 57.

(16) Fehlner, T. P.; Calvo-Perez, V.; Cen, W. *J. Electron Spectr.* **1993**, *66*, 29.

(17) Cen, W. Ph.D. Thesis, University of Notre Dame, Notre Dame, IN, 1992.

(18) Bañares, M. A.; Dauphin, L.; Calvo-Perez, V.; Fehlner, T. P.; Wolf, E. E. *J. Catal.* **1995**, *152*, 396.

(19) Bañares, M.; Patil, A. N.; Fehlner, T. P.; Wolf, E. E. *Catal. Lett.* **1995**, *34*, 251.

(20) Stutte, B.; Bätzel, V.; Boese, R.; Schmid, G. *Chem. Ber.* **1978**, *111*, 1603.

S0276-7333(97)00837-6 CCC: $14.00

similar uses for related cluster assemblies utilizing the tricobalt cluster with a different functional group.[22]

In the present work, we have investigated the reaction of $(CO)_9Co_3(\mu_3\text{-}CCOOH)$ with titanium and zirconium alkoxides. Metal alkoxide chemistry itself continues to draw attention as these compounds serve as precursors for the formation of oxide networks via inorganic polymerization reactions.[23,24] Isolation of network compounds of medium size have produced models for large network molecules, e.g., the structural characterization of $Ti_{16}O_{16}(OC_2H_5)_{32}$.[25] Spectroscopic studies, e.g., ^{17}O NMR, have provided information on oxoalkoxides in solution.[26−31] The addition of organic acids modifies network formation and permits the isolation of species such as $Ti_6O_4(OR)_8(CH_3CO_2)_8$ and related compounds.[32−36] The same should be possible for zirconium; however, there is only one report of a related Zr(IV) oxocarboxylate but none of a simple Zr(IV) alkoxycarboxylate.[37] The formal replacement of an organic group with the $(CO)_9Co_3(\mu_3\text{-}C-)$ group on the acid introduces a large substituent with very different electronic properties, and an examination of the consequences of these differences is the subject of this study.[38]

Experimental Section

General. All operations were conducted under a dinitrogen atmosphere using standard Schlenk techniques.[39] Solvents were distilled before use under N_2 as follows: sodium benzophenone ketyl for hexane, diethyl ether, and tetrahydrofuran; P_2O_5 for CH_2Cl_2; manganese metal for CH_3OH. Regent-grade acetone, $Cl_3CC(O)OEt$, $(CH_3)_2CHOH$, and absolute ethanol were used as received. KBr, $M(OR)_4$ ($M = Ti$; $R = -CH_3, -CH_2CH_3, -CH(CH_3)_2, -CH_2CH_2CH_2CH_3$; $M = Zr$, $R = -CH(CH_3)_2$), phenol, 2,6-dimethylphenol, catechol, and $CH_3C(CH_2OH)_3$ were used as received from Aldrich. Likewise, $Co_2(CO)_8$ (Strem) was used as received. $(CO)_9Co_3(\mu_3\text{-}CCO_2H)$ was prepared by a modified literature method.[9,15,40,41] FT-IR spectra were measured on Nicolet 205 FT-IR. UV−Vis spectra were recorded on a Varian Cary-3 UV−vis spectrophotometer. NMR spectra were recorded on a 300 MHz Varian or GE GN 300 FT-NMR spectrometer, and solvent signals were used as a reference. The cyclic voltammograms were run on a PAR model 173 potentiostat with a model 175 universal programmer and model 179 digital coulometer. A single compartment cell with a three-electrode system consisting of a Ag/AgCl reference, a platinum wire auxiliary, and a platinum working electrode was employed. The solvent was CH_2Cl_2 with 0.1 M $(Bu_4N)ClO_4$ as the supporting electrolyte. Elemental analyses were performed by Galbraith Laboratories, Knoxville, TN, and M-H-W Laboratories, Phoenix, AZ.

$Zr_2(\mu\text{-}OCH(CH_3)_2)_2(OCH(CH_3)_2)_2\{\mu\text{-}(CO)_9Co_3(\mu_3\text{-}CCO_2)\}_2\text{-}\{(CO)_9Co_3(\mu_3\text{-}CCO_2)\}_2$, 1. $(CO)_9Co_3(\mu_3\text{-}CCO_2H)$ (2 mmol, 0.97 g) was loaded into a 50 mL Schlenk flask equipped with a rubber septum and a magnetic stirring bar. This flask had been evacuated and refilled with dinitrogen several times before 20 mL of THF was added to the flask via syringe with rapid stirring. After all of the solid was dissolved, 0.387 g of $[Zr(OCH(CH_3)_2)_4\cdot HOCH(CH_3)_2]_2$ (0.5 mmol) in 10 mL of toluene was added to the solution by syringe. The solution was stirred for 10 h at 50 °C to give a purple solution. The solvents were removed *in vacuo*. The microcrystals obtained were washed with CH_2Cl_2 to yield 900 mg of black crystals. Recrystallization from a solution of mixed THF/toluene layered by isopropyl alcohol produced large crystals suitable for X-ray diffraction. The crystals are slightly soluble in THF, toluene, and CH_2Cl_2 and insoluble in isopropyl alcohol and hexane. Total yield is 80% based on the total amount of Zr.

Spectroscopic and analytical data: ^1H NMR (C_6D_6, 20 °C, δ) 3.653 (1H, m, $OCH(CH_3)_2$) 0.937 (6H, d, $OCH(CH_3)_2$); IR (KBr, cm^{-1}) 2111 (s), 2055 (vs, sh), 2044 (vs), 1523 (w), 1464 (vw), 1455 (w), 1413 (m), 1378 (s), 1337 (w, sh), 1166 (w, sh), 1143 (w), 1114 (w), 1022 (w), 944 (w), 803 (w), 797 (w), 747 (m), 725 (m), 705 (w, sh), 551 (w), 529 (m), 501 (s), 474 (w), 463 (w). Anal. Calcd for $Zr_2Co_{12}O_{48}C_{56}H_{28}$: C, 28.52; H, 1.20. Found: C, 28.68; H, 1.26.

$Ti_4(\mu_3\text{-}O)_4(OCH(CH_3)_2)_4\{\mu\text{-}(CO)_9Co_3(\mu_3\text{-}CCO_2)\}_4$, 2a. A solution of $(CO)_9Co_3(\mu_3\text{-}CCO_2H)$ (2 mmol, 0.97 g) in 30 mL of THF in a 50 mL Schlenk flask was prepared as described for **1**. $Ti(OCH(CH_3)_2)_4$ (1 mmol, 0.31 mL), was added by syringe and, after stirring for 20 h at room temperature, gave a purple solution. The solution was evaporated to dryness, and the remaining solid was dissolved in 20 mL of CH_2Cl_2. The purple solution was layered by isopropyl alcohol and kept at 4 °C for 1 week. After standing at −20 °C for several days, column-like crystals appeared on the bottom of the flask. The crystals were collected and washed with isopropyl alcohol to give 250 mg of the product. The solution was dried, and the solid obtained was extracted by toluene. The toluene solution was layered with isopropyl alcohol. The flask was kept at 4 °C for 1 week and then at −20 °C. The second batch of crystals gave 200 mg of additional product. The crystals are soluble in THF, toluene, acetone, CH_2Cl_2, and hexane but insoluble in isopropyl alcohol. Total yield is 74% based on the amount Ti.

Spectroscopic and analytical data: ^1H NMR (C_6D_6, 20 °C, δ) 4.832 (sept, 1H, $J_{HH} = 6.3$ Hz, $CH(CH_3)_2$), 1.462 (d, 6H, $J_{HH} = 6.6$ Hz, $CH(CH_3)_2$); $^{13}C\{H\}$ NMR (C_6D_6, 20 °C, δ) 198.7 (CO), 188.6 (COO), 80.2 ($CH(CH_3)_2$), 24.5 ($CH(CH_3)_2$); IR (KBr, cm^{-1}) 2111 (m), 2050 (vs), 2037 (vs, sh), 1510 (m), 1488 (m), 1383 (s), 1341 (m, sh), 1128 (m), 1007 (m), 726 (m), 620 (m), 612 (m), 568 (w), 529 (m), 498 (m), 465 (w); Solution IR (C_6D_6, 20 °C, cm^{-1}) 2110 (m), 2068 (vs), 2043 (vs), 1510 (w), 1488 (w), 1384 (s); UV−vis (hexane) (λ, nm (ϵ, $cm^{-1}M^{-1}$)) 375 (sh, 15 700),

---

[21] Chao, L. C. F.; Decken, A.; Britten, J. F.; McGlinchey, M. J. *Can. J. Chem.* **1995**, *73*, 1196.

[22] Ritter, U.; Winkhofer, N.; Murugavel, R.; Voigt, A.; Stalke, D.; Roesky, H. W. *J. Am. Chem. Soc.* **1996**, *118*, 8580.

[23] Chandler, C. D.; Roger, C.; Hampden-Smith, M. J. *Chem. Rev.* **1993**, *93*, 1205.

[24] *Ultrastructure Processing of Ceramic, Glasses and Composites*; Hench, L. L.; Ulrich, D. R., Eds.; Wiley: New York, 1984.

[25] Schmid, R.; Mosset, A.; Galy, J. *J. Chem. Soc., Dalton Trans.* **1991**, 1999.

[26] Day, V. W.; Eberspacher, T. A.; Klemperer, W. G.; Park, C. W. *J. Am. Chem. Soc.* **1993**, *115*, 8469.

[27] Day, V. W.; Eberspacher, T. A.; Chen, Y.; Hao, J.; Klemperer, W. G. *Inorg. Chim. Acta* **1995**, *229*, 391.

[28] Chen, Y. W.; Klemperer, W. G.; Park, C. W. *Mater. Res. Symp. Proc.* **1992**, *271*, 57.

[29] Day, V. W.; Eberspacher, T. A.; Klemperer, W. G.; Park, C. W.; Rosenberg, F. S. *J. Am. Chem. Soc.* **1991**, *113*, 8190.

[30] Charnick, S. G.; Klemperer, W. *Abstracts of Papers*, 208th National Meeting of the American Chemical Society, Washington, DC, Fall 1994; American Chemical Society: Washington, DC, 1994; pp I 393.

[31] Chen, Y. W.; Klemperer, W. G. *Abstracts of Papers*, 209th National Meeting of the American Chemical Society, Anaheim, CA, Spring 1995; American Chemical Society: Washington, DC, 1995; pp I 169.

[32] Doeuff, S.; Dromzee, Y.; Taulelle, F.; Sanchez, C. *Inorg. Chem.* **1989**, *28*, 4439.

[33] Doeuff, S.; Dromzee, Y.; Sanchez, C. *C. R. Acad. Sci. Paris, Ser. II* **1989**, *308*, 1409.

[34] Boyle, T. J.; Schwartz, R. W. *Comm. Inorg. Chem.* **1994**, *16*, 243.

[35] Gautier-Luneau, I.; Mosset, A.; Galy, J. *Z. Kristallogr.* **1987**, *180*, 83.

[36] Toledano, P.; In, M.; Sanchez, C. *C. C. R. Acad. Sci. Paris, Ser. II* **1991**, *313*, 1247.

[37] Kickelbick, G.; Schubert, U. *Chem. Ber./Recl.* **1997**, *130*, 473.

[38] Lei, X.; Shang, M.; Fehlner, T. P. *Organometallics* **1996**, *15*, 3779.

[39] Shriver, D. F.; Drezdzon, M. A. *The Manipulation of Air Sensitive Compounds*, 2nd ed.; Wiley-Interscience: New York, 1986.

[40] Seyferth, D.; Hallgren, J. E.; Hung, P. L. K. *J. Organomet. Chem.* **1973**, *50*, 265.

[41] Cen, W.; Haller, K. J.; Fehlner, T. P. *Inorg. Chem.* **1993**, *32*, 995.

515 (5500); CV (V, Ag/AgCl) $E_{1/2}$ −0.81, ΔE 0.36. Anal. Calcd for $Ti_4Co_{12}O_{52}C_{56}H_{28}$: C, 27.66; H, 1.16. Found: C, 27.80; H, 1.11.

$Ti_4(\mu_3\text{-}O)_4(O(CH_2)_3CH_3)_4\{\mu\text{-}(CO)_9Co_3(\mu_3\text{-}CCO_2)\}_4$, 2b. A solution of $(CO)_9Co_3(\mu_3\text{-}CCO_2H)$ (2 mmol, 0.97 g) in 20 mL of THF in a 100 mL Schlenk flask was prepared as for **1**. $Ti(O(CH_2)_3CH_3)_4$ (1 mmol, 0.34 mL), was added by syringe, and the reaction mixture was stirred for 5 h at 50 °C to give a purple solution. THF was removed under vacuum, and 25 mL of hexane was added to the residue. The mixture was stirred overnight at room temperature and then filtered through a funnel with 2 mm of Celite under N_2. The filtrate was kept at 4 °C for 1 week. Large black crystals were collected, washed with isopropyl alcohol and dried *in vacuo*. Total yield is ca. 65% based on the amount of Ti. The compound is soluble in hexane, toluene, acetone, THF, and CH_2Cl_2.

Spectroscopic and analytical data: ^1H NMR (C_6D_6, 20 °C, δ) 4.532 (t, 2H, $J_{HH} = 6.4$ Hz, $OCH_2CH_2CH_2CH_3$), 1.760 (m, 2H, $OCH_2CH_2CH_2CH_3$), 1.589 (m, 2H, $OCH_2CH_2CH_2CH_3$), 1.049 (t, 3H, $J_{HH} = 7.3$ Hz, $OCH_2CH_2CH_2CH_3$); ^{13}C {H} NMR (C_6D_6, 20 °C, δ) 199.0 (*C*O), 188.4 (*C*OO), 78.3 ($OCH_2CH_2CH_2CH_3$), 35.2 ($OCH_2CH_2CH_2CH_3$), 19.4 ($OCH_2CH_2CH_2CH_3$), 14.0 ($O(CH_2)_3CH_3$); IR (KBr, cm^{-1}) 2110 (s), 2059 (vs), 2044 (vs), 1511 (m), 1489 (m), 1382 (s), 1340 (m, sh), 1126 (m), 1096 (m), 1039 (w), 727 (s), 620 (s, sh), 617 (s), 565 (m), 529 (s), 499 (s), 462 (m), 406 (s); Solution IR (C_6D_6, 20 °C, cm^{-1}) 2110 (s), 2068 (vs), 2043 (vs), 1510 (w), 1488 (w), 1382 (s), 1126 (w), 1097 (m), 1039 (w); UV−vis (hexane) (λ, nm (ϵ, cm^{-1} M^{-1})) 372 (sh, 27 600), 514 (5800). Anal. Calcd for $Ti_4Co_{12}O_{52}C_{60}H_{36}$: C, 28.97; H, 1.46. Found: C, 29.04; H, 1.48.

$Ti_4(\mu_3\text{-}O)_4(OC_6H_5)_4\{\mu\text{-}(CO)_9Co_3(\mu_3\text{-}CCO_2)\}_4\cdot HOC_6H_5$, 2c. C_6H_5OH (4 mmol, 0.376 g) and 20 mL of toluene in a 100 mL Schlenk flask was prepared as described for **1**. After the mixture was stirred at 50 °C for 1 h, 0.155 mL (0.5 mmol) of $Ti(OCH(CH_3)_2)_4$ was added dropwise. The color of the solution immediately changed to yellow and then to orange. The solution was dried under vacuum to yield an orange solid. A mixed solvent mixture of THF/tol (20 mL; v:v, 1:1) was put into the flask to dissolve the solid. After all of the solid was dissolved at 50 °C, 0.488 g of $(CO)_9Co_3(\mu_3\text{-}CCO_2H)$ (1 mmol) was added. The slurry was stirred overnight to give a purple solution. The solvent was removed under vacuum to generate a brown oil, which was dissolved in 20 mL of hexane. The hexane solution was filtered through a funnel with 2 mm of Celite under N_2, and the filtrate was kept undisturbed overnight at room temperature. Black polyhedron crystals appeared on the bottom of the flask. The yield is 60% based on the amount of Ti. The compound is soluble in hexane, toluene, acetone, diethyl ether, THF, and CH_2Cl_2.

Spectroscopic and analytical data: ^1H NMR (CD_3COCD_3, 20 °C, δ) 7.120−7.198 (m, 5H, C_6H_5OH), 6.761−7.021 (m, 20H, $-OC_6H_5$); IR (KBr, cm^{-1}) 2111 (s), 2062 (vs), 2045 (vs), 1589 (w), 1475 (s), 1379 (s), 1341 (m, sh), 1249 (s), 1162 (w), 1093 (w), 898 (s), 755 (m), 728 (m), 688 (w), 666 (m), 612 (s), 566 (m), 527 (m), 498 (s), 462 (m), 408 (s); Solution IR (C_6D_6, 20 °C, cm^{-1}) 2111 (s), 2070 (vs), 2046 (vs), 1590 (w), 1475 (s), 1379 (s), 1342 (w), 1332 (m), 1259 (s), 1162 (w), 1094 (m), 1021 (m); UV−vis (hexane) (λ, nm (ϵ, cm^{-1} M^{-1})) 375 (sh, 39 300). Anal. Calcd for $Ti_4Co_{12}O_{53}C_{74}H_{21}$: C, 33.06; H, 0.79. Found: C, 33.16; H, 0.90.

$[Ti_4(\mu_3\text{-}O)_4(2,6\text{-}(CH_3)_2\text{-}OC_6H_3)_4\{\mu\text{-}(CO)_9Co_3(\mu_3\text{-}CCO_2)\}_4]\cdot C_6H_{14}$, 2d. 2,6-Dimethylphenol (4 mmol, 0.488 g) and 10 mL of CH_2Cl_2 in a 100 mL Schlenk was prepared as for **1**. After the mixture was stirred for 10 min, 0.155 mL (0.5 mmol) of $Ti(OCH(CH_3)_2)_4$ was added dropwise. The color immediately changed to yellow but was stirred for an additional 10 min. Evacuating the reaction flask for 1 h led to some white crystals on the upper part of the flask and a yellow gel on the bottom. Toluene (30 mL) was added to the flask to afford a yellow solution. $(CO)_9Co_3(\mu_3\text{-}CCO_2H)$ (1 mmol, 0.448 g) was added, and the slurry was stirred for 6 h at 50 °C to give a yellowish-brown solution. The solvent was removed under vacuum to generate an orange-brown oil, which was dissolved in 20 mL of hexane. The hexane solution was kept undisturbed for several days at room temperature, and black polyhedral crystals appeared on the bottom of the flask. Total yield is ca. 80% based on the amount of Ti. The compound is soluble in hexane, toluene, acetone, diethyl ether, THF, CH_2Cl_2, and cyclohexane.

Spectroscopic and analytical data: ^1H NMR (CD_3COCD_3, 20 °C, δ) 6.144 (d, 2H, *para-H*, 2.6-$(CH_3)_2$-OC_6H_3), 6.001 (t, 1H, *meta-H*, 2.6-$(CH_3)_2$-OC_6H_3), 2.040 (s, 6H, 2.6-$(CH_3)_2$-OC_6H_3), 0.882 (m, hexane); IR (KBr, cm^{-1}) 2111 (s), 2063 (vs), 2045 (vs), 1494 (m), 1465 (s), 1372 (vs), 1335 (s, sh), 1268 (m), 1219 (s), 1089 (w), 915 (s), 760 (m), 738 (s), 728 (s), 609 (s), 587 (s), 568 (m), 556 (m), 525 (m), 498 (s), 456 (m), 406 (s); Solution IR (C_6D_6, 20 °C, cm^{-1}) 2111 (s), 2070 (vs), 2046 (vs), 1590 (w), 1475 (s), 1379 (s), 1342 (w), 1332 (m), 1259 (s), 1162 (w), 1094 (m), 1021 (m); UV−vis (hexane) (λ, nm (ϵ, cm^{-1} M^{-1})) 380 (sh, 30 400); CV (V, Ag/AgCl) $E_{1/2}$ −0.71, ΔE 0.26. Anal. Calcd for $Ti_4Co_{12}O_{52}C_{82}H_{50}$: C, 35.61; H, 1.82. Found: C, 35.90; H, 1.79.

$Ti_6(\mu_3\text{-}O)_4(\mu\text{-}OCH_2CH_3)_4(OCH_2CH_3)_8\{\mu\text{-}(CO)_9Co_3(\mu_3\text{-}CCO_2)\}_4$, 3. A solution of $(CO)_9Co_3(\mu_3\text{-}CCO_2H)$ (2 mmol, 0.97 g) in 30 mL of THF in a 40 mL Schlenk flask was prepared as for **1**. $Ti(OCH_2CH_3)_4$ (1 mmol, 0.22 mL) was added, and the reaction mixture was stirred for 12 h at room temperature to give a purple solution. THF was removed under vacuum. The solid obtained was dissolved in 20 mL of CH_2Cl_2, and 10 mL of EtOH was added to the purple solution. The flask was kept at 4 °C for 1 week to yield black column-like crystals. The crystals were collected and washed with ethanol to afford 200 mg of the product. The mother solution was kept at −20 °C, and a second crop yielded an additional 150 mg of product. The crystals are soluble in THF, toluene, and CH_2Cl_2 but are insoluble in hexane. The yield is 70% based on the amount of Ti.

Spectroscopic and analytical data: ^1H NMR (C_6D_6, 20 °C, δ) 4.493 (q, 2H, $-CH_2CH_3$), 1.345 (t, 3H, $-CH_2CH_3$); ^{13}C {^1H} NMR (C_6D_6, 20 °C, δ) 199.0 (*C*O), 188.6 (*C*OO), 73.9 ($-CH_2$-CH_3), 18.1 ($-CH_2CH_3$); IR (KBr, cm^{-1}) 2110 (m), 2054 (vs), 2045 (vs, sh), 1513 (w), 1490 (w), 1378 (m), 1340 (w, sh), 1123 (m), 1101 (w, sh), 1073 (w), 723 (m), 620 (m), 612 (m, sh), 553 (w), 530 (m), 499 (m); Solution IR (CH_2Cl_2, 20 °C, cm^{-1}) 2110 (s), 2069 (vs), 2044 (vs), 1510 (w), 1505 (w), 1485 (w), 1379 (s), 1338 (w); UV−vis (CH_2Cl_2) (λ, nm (ϵ, cm^{-1} M^{-1})) 370 (sh, 30 200), 515 (6400); CV (V, Ag/AgCl) $E_{1/2}$ −0.88, ΔE 0.22. Anal. Calcd for $Ti_6Co_{12}O_{60}C_{68}H_{60}$: C, 28.84; H, 2.14. Found: C, 29.00; H, 1.98.

$[Ti_6(\mu_3\text{-}O)_2)(\mu\text{-}O)_2(\mu\text{-}OCH(CH_3)_2)_2(OCH(CH_3)_2)_2(1,2\text{-}O_2C_6H_4)_4\{\mu\text{-}(CO)_9Co_3(\mu_3\text{-}CCO_2)\}_4]$, 4. To a solution of 0.055 g (0.5 mmol) of catechol in 20 mL of toluene was added 0.155 mL (0.5 mmol) of $Ti(OCH(CH_3)_2)_4$ under rapid stirring at 50 °C. The solution immediately changed from colorless to red, and 30 min later, 10 mL of THF and 0.488 g of $(CO)_9Co_3(\mu_3\text{-}CCO_2H)$ (1 mmol) were added. The reaction mixture became dark red. After the mixture was stirred at 50 °C overnight, all solvents were removed under vacuum and the black oil was extracted with CH_2Cl_2 to afford a red-brown solution, which was filtered through a funnel containing 2 mm of Celite. The solution obtained was layered with hexane. Black crystals were produced and washed with hexane. The crystals are soluble in THF, toluene, and CH_2Cl_2 but are insoluble in hexane. The yield is 45% based on the amount of Ti.

Spectroscopic and analytical data: IR (KBr, cm^{-1}) 2111 (s), 2061 (vs), 2048 (vs), 1485 (m), 1473 (w), 1369 (m), 1331 (m), 1256 (m), 1113 (m), 1110 (m), 1112 (w), 851 (m), 829 (m), 807 (s), 740 (s), 724 (s), 655 (s), 628 (s), 604 (w), 550 (m), 526 (m), 498 (s), 409 (s); Solution IR (CH_2Cl_2, 20 °C, cm^{-1}) 2110 (w), 2067 (vs), 2046 (vs), 1376 (w); UV−vis (CH_2Cl_2) (λ, nm (ϵ, cm^{-1} M^{-1})) 387 (sh, 23 400), 515 (6800). Anal. Calcd for $Ti_6Co_{12}O_{60}C_{80}H_{44}$: C, 32.46; H, 1.50. Found: C, 33.77; H, 1.49.

$[Ti_2Co_2\{(OCH_2)_3CCH_3\}_2(OCH(CH_3)_2)_2\{\mu\text{-}(CO)_9Co_3(\mu_3\text{-}CCO_2)\}_4]$, 5. $(HOCH_2)_3CCH_3$ (0.060 g, 0.5 mmol) and 10 mL

Table 1. Crystallographic Data for 1, 2a, 2b, 2c·HOC_6H_5, and 2d·C_6H_{14}

	1	**2a**	**2b**	**2c**·HOC_6H_5	**2d**·C_6H_{14}
empirical formula	$C_{56}H_{28}Co_{12}O_{48}Zr_2$	$C_{56}H_{28}Co_{12}O_{52}Ti_4$	$C_{60}H_{36}Co_{12}O_{52}Ti_4$	$C_{74}H_{26}Co_{12}O_{53}Ti_4$	$C_{82}H_{50}Co_{12}O_{52}Ti_4$
fw	2358.38	2431.54	2487.65	2661.71	2765.98
cryst size, mm	0.50 × 0.32 × 0.12	0.20 × 0.20 × 0.15	0.48 × 0.28 × 0.28	0.30 × 0.25 × 0.19	0.31 × 0.28 × 0.25
λ (Mo Kα), Å	0.710 73	0.710 73	0.710 73	0.710 73	0.710 73
cryst syst	triclinic	monoclinic	monoclinic	monoclinic	monoclinic
space group	$P\bar{1}$	$C2/c$	$C2/c$	$P2_1/c$	$C2/c$
a, Å	15.889(2)	15.193(3)	15.5751(8)	13.560(3)	21.939(2)
b, Å	19.480(3)	19.138(3)	20.4838(13)	48.679(4)	16.311(2)
c, Å	28.258(3)	29.008(4)	28.9598(13)	16.031(3)	30.200(3)
α, deg	89.499(9)				
β, deg	82.819(8)	92.08(3)	91.431(4)	111.28(2)	90.321(8)
γ, deg	73.510(10)				
volume, Å^3	8313(2)	8429(2)	9236.4(9)	9860(3)	10807(2)
Z	4	4	4	4	4
temperature, K	293(2)	130(2)	293(2)	293(2)	293(2)
D_{calcd}, Mg/m^3	1.883	1.916	1.789	1.793	1.700
μ (Mo Kα), mm^{-1}	2.659	2.748	2.510	2.359	2.155
no. of unique data	21 665	8430	6444	12 832	7035
no. of obsd data ($I > 2\sigma(I)$)	16 450	7108	4511	7753	4229
no. of variables	2181	615	588	1342	711
goodness-of-fit on F^2	1.134	1.069	1.121	1.166	1.196
R1,[a] wR2[b] ($I > 2\sigma(I)$)	0.0404, 0.0888	0.0413, 0.0919	0.0533, 0.1341	0.0596, 0.1213	0.1149, 0.2714
R1,[a] wR2[b] (all data)	0.0718, 0.1327	0.0530, 0.0994	0.0897, 0.1705	0.1373, 0.1729	0.1882, 0.3779

[a] $R1 = \sum||F_o| - |F_c||/\sum|F_o|$. [b] $wR2 = [\sum w(F_o^2 - F_c^2)^2/\sum(w|F_o|^2)^2]^{1/2}$.

of THF in a 100 mL Schlenk flask was prepared as for **1**. After the mixture was stirred at 50 °C for 10 h, 0.155 mL (0.5 mmol) of $Ti(OCH(CH_3)_2)_4$ was added dropwise, imparting a pale yellow to the solution. After the mixture was stirred for 6 h at 50 °C, the solvent was removed under vacuum to yield a light yellow solid. THF (20 mL) was added, after the solid was dissolved at 50 °C, 0.488 g of$(CO)_9Co_3(\mu_3\text{-}CCO_2H)$ (1 mmol) was added. The slurry was stirred overnight at 50 °C to give a purple solution. Removal of the solvent under vacuum generated brown microcrystals, which were dissolved in 10 mL of THF. The THF solution was filtered through a funnel with 4 mm of Celite under N_2, and the filtrate was kept undisturbed overnight at room temperature for 2 days. After the mixture was cooled at 4 °C for 2 more days, black block-like crystals appeared on the bottom of the flask. The total yield is ca. 40% based on the amount of Ti. The crystals are slightly soluble in THF and CH_2Cl_2.

Spectroscopic and analytical data: IR (KBr, cm^{-1}) 2107 (s), 2051 (vs), 2041 (vs), 1509 (s), 1466 (w), 1364 (s), 1330 (w), 1316 (m, sh), 1163 (w), 1129 (s), 1067 (s), 1044 (m), 1021 (s), 1005 (m), 748 (s), 716 (s), 625 (s), 552 (s), 530 (s), 498 (s), 473 (m, sh), 443 (w), 498 (s), 473 (m, sh), 443 (w); UV−vis (CH_2Cl_2) (λ, nm (ϵ, cm^{-1} M^{-1})) 385 (sh, 18 200), 515 (7200). Anal. Calcd for $Ti_2Co_{14}O_{52}C_{60}H_{32}$: C, 28.76; H, 1.29. Found: C, 28.73; H, 1.39.

$[\{Co_3Ti(OCH_3)_6(HOCH_3)(THF)\{\mu\text{-}(CO)_9Co_3(\mu_3\text{-}CCO_2)\}_3\}_2\text{-}(O_2CCO_2)]\cdot 2HOCH_3\cdot 2THF$, 6. $(CO)_9Co_3(\mu_3\text{-}CCO_2H)$ (1 mmol, 0.488 g) and $Ti(OCH_3)_4$ (1 mmol, 0.172 g) were loaded into a 100 mL Schlenk flask equipped with a rubber septum and a magnetic stirring bar. THF (30 mL) was added to the flask via syringe, and the reaction mixture was stirred for 20 h at 45 °C to give a purple solution. THF was removed under vacuum, and the resulting black microcrystals were dissolved in 15 mL of THF. The red-brown solution obtained was layered with CH_3OH. After several days, red-brown platelike crystals appeared on the wall of the flask. The yield is ca. 35% based on the amount of Ti. The crystals are slightly soluble in THF and CH_2Cl_2 and insoluble in hexane and methanol.

Spectroscopic and analytical data: IR (KBr, cm^{-1}) 2108 (m), 2045 (vs), 1655 (m), 1541 (w, br), 1368 (m), 1338 (m, sh), 1138 (w), 1088 (w, br), 1023 (m), 797 (w), 752 (w), 714 (w), 581 (w), 550 (m), 530 (m), 501 (s); UV−vis (CH_2Cl_2) (λ, nm (ϵ, cm^{-1} M^{-1})) 388 (sh, 9200), 526 (5100). Anal. Calcd for $Ti_2Co_{24}O_{86}C_{90}H_{60}$: C, 26.84; H, 1.50. Found: C, 25.38; H, 1.20.

Structure Determinations. General. The X-ray diffraction data were collected either on an Enraf-Nonius CAD4 diffractometer equipped with graphite-crystal-monochromated Mo Kα radiation at room temperature or an Enraf-Nonius FAST area-detector diffractometer at low temperature. In the former case, Lorentz and polarization corrections were applied to the data. An empirical absorption correction based on a series of ψ-scans was also applied to the data. In the latter case, data were collected at 130 K with a Mo rotating anode source ($\lambda = 0.710\ 73$ Å). The MADNES package was employed for cell constant determination, image measurement, and intensity data evaluation. The detailed procedure for small molecules using an area detector has been described elsewhere.[42] Each structure was solved by either the MULTAN direct methods of the SDP package[43] or the SHELXS-86 program[44] followed by successive difference Fourier syntheses. Metal atoms were located from an E-map. The remaining atoms were found in succeeding difference Fourier syntheses. Preliminary least-squares refinement was performed with the SDP package, and further full-matrix least-squares refinements were carried out by using the SHELXL-93 program[44] based on F^2 for all reflections. Crystal data for **1** to **6** are given in Tables 1 and 2. Specific details for each structure follow.

$Zr_2(\mu\text{-}OCH(CH_3)_2)_2(OCH(CH_3)_2)_2\{\mu\text{-}(CO)_9Co_3(\mu_3\text{-}CCO_2)\}_2\text{-}\{(CO)_9Co_3(\mu_3\text{-}CCO_2)\}_2$, 1. A black column-like crystal was mounted on the top of a glass fiber, and data were collected on the CAD4 diffractometer. There are two molecules in an asymmetric unit. One of the tricobalt fragments in each molecule is disordered. The site occupancy factor for each of the tricobalt units was refined. The final thermal parameters for these disordered atoms were reasonable. Hydrogen atoms were included in the refinement but idealized to ride on the atom to which they are bonded. All non-hydrogen atoms were refined with anisotropic thermal parameters in the final cycle, $R1 = 0.0404$ for 16 450 observed unique reflections with $I > 2\sigma(I)$ and $wR2(F^2) = 0.1327$ for all data (2176 variables refined). Selected distances and angles are given in Table 3.

$Ti_4(\mu_3\text{-}O)_4(OCH(CH_3)_2)_4\{\mu\text{-}(CO)_9Co_3(\mu_3\text{-}CCO_2)\}_4$, 2a. A black column-like crystal was mounted on the top of a glass fiber, and data were collected on the FAST diffractometer. No absorption correction was made. All non-hydrogen atoms were refined with anisotropic thermal parameters, and hydrogen

---

(42) Scheidt, W. R.; Turowska-Tyrk, I. *Inorg. Chem.* **1994**, *33*, 1314.

(43) Frenz, B. A. In *The Enraf-Nonius CAD4-A Real-time System for Concurrent X-ray Data Collection and Crystal Structure Determination*; Schenk, H., Olthof-Hazelkamp, R., von Konigsveld, H., Bassi, G. C., Eds.; Delft University Press: Delft, Holland, 1978; pp 64.

(44) Sheldrick, G. M. *SHELXL Version 5*; Siemens Industrial Automation, Inc.: Madison, WI, 1994.

Table 2. Crystallographic Data for 3, 4, 5, and 6·2HOCH$_3$·2THF

	3	**4**	**5**	**6**·2HOCH$_3$·2THF
empirical formula	$C_{68}H_{60}Co_{12}O_{60}Ti_6$	$C_{80}H_{44}Co_{12}O_{60}Ti_6$	$C_{60}H_{32}Co_{14}O_{52}Ti_2$	$C_{100}H_{84}Co_{24}O_{90}Ti_2$
fw	2831.72	2959.71	2505.68	4235.79
cryst size, mm	0.55 × 0.20 × 0.15	0.15 × 0.07 × 0.03	0.45 × 0.28 × 0.15	0.15 × 0.10 × 0.03
λ (Mo Kα), Å	0.71073	0.71073	0.71073	0.71073
cryst syst	monoclinic	triclinic	monoclinic	triclinic
space group	$P2_1/c$	$P\bar{1}$	$P2_1/c$	$P\bar{1}$
a, Å	15.814(2)	11.6126(9)	15.180(4)	12.115(3)
b, Å	16.215(2)	14.482(2)	21.579(5)	17.947(6)
c, Å	21.149(3)	17.865(3)	15.305(5)	19.819(2)
α, deg		109.391(12)		64.82(4)
β, deg	92.718(12)	94.873(6)	114.71(2)	77.39(2)
γ, deg		106.593(10)		73.41(2)
volume, Å^3	5417(1)	2661.7(6)	4554(2)	3714(2)
Z	2	1	2	1
temperature, K	293(2)	130(2)	293(2)	130(2)
D_{calcd}, Mg/m^3	1.736	1.846	1.827	1.894
μ (Mo Kα), mm^{-1}	2.291	2.336	2.734	2.803
no. of unique data	7519	13419	6335	18826
no. of obsd data($I > 2\sigma(I)$)	5286	10160	4880	9073
no. of variables	697	712	577	977
goodness-of-fit on F^2	1.135	1.048	1.106	1.002
R1,[a] wR2[b] ($I > 2\sigma(I)$)	0.0527, 0.1319	0.0489, 0.0943	0.0515, 0.1265	0.0843, 0.1560
R1,[a] wR2[b] (all data)	0.0931, 0.1667	0.0755, 0.1051	0.0711, 0.1493	0.1895, 0.2159

[a] SHELXL R1 = $\sum||F_o| - |F_c||/\sum|F_o|$. [b] wR2 = $[\sum w(F_o{}^2 - F_c{}^2)^2/\sum(w|F_o|^2)^2]^{1/2}$.

Table 3. Selected Bond Lengths (Å) and Angles (deg) for 1

Zr(1)···Zr(2)	3.3503(9)	Zr(2)−O(12)	2.186(4)
Zr(1)−O(11)	2.192(4)	Zr(2)−O(22)	2.205(4)
Zr(1)−O(21)	2.189(4)	Zr(2)−O(41)	2.254(4)
Zr(1)−O(31)	2.258(4)	Zr(2)−O(42)	2.249(4)
Zr(1)−O(32)	2.264(4)	Zr(2)−O(101)	2.161(4)
Zr(1)−O(101)	2.146(4)	Zr(2)−O(201)	2.153(4)
Zr(1)−O(201)	2.158(4)	Zr(2)−O(401)	1.893(4)
Zr(1)−O(301)	1.896 (4)		
O(11)−Zr(1)−O(32)	73.6(2)	O(12)−Zr(2)−O(41)	72.5(2)
O(11)−Zr(1)−O(201)	76.5(2)	O(12)−Zr(2)−O(101)	76.7(2)
O(21)−Zr(1)−O(31)	73.4(2)	O(22)−Zr(2)−O(101)	76.3(2)
O(21)−Zr(1)−O(101)	80.4(2)	O(22)−Zr(2)−O(42)	74.7(2)
O(31)−Zr(1)−O(32)	57.0(2)	O(41)−Zr(2)−O(42)	57.5(2)
O(101)−Zr(1)−O(301)	175.8(2)	O(201)−Zr(2)−O(401)	175.2(2)
Zr(1)−O(101)−Zr(2)	102.1(2)	Zr(1)−O(201)−Zr(2)	102.0(2)

atoms were refined with isotropic thermal parameters in the final cycle, R1 = 0.0413 for 7108 observed unique reflections with $I > 2\sigma(I)$ and wR2(F^2) = 0.0994 for all data (615 variables refined).

Ti$_4$(μ_3-O)$_4$(O(CH$_2$)$_3$CH$_3$)$_4${μ-(CO)$_9$Co$_3$(μ_3-CCO$_2$)}$_4$, 2b. A black column-like crystal was mounted on the top of a glass fiber, and data were collected on the CAD4 diffractometer. A difference map revealed that the butoxide and one of the tricobalt groups were disordered. The occupancies and displacement parameters of these atoms were refined with fractional site occupancies. One of the tricobalt units was disordered and refined with fractional site occupancies. The two carbon chains of the butoxy group were also disordered, and the occupancies and displacement parameters of the disordered carbon atoms were refined. All non-hydrogen atoms were refined with anisotropic thermal parameters except for these restrained atoms in the final cycle, R1 = 0.0533 for 3718 observed unique reflections with $I > 2\sigma(I)$ and wR2(F^2) = 0.1758 for all data (588 variables refined).

Ti$_4$(μ_3-O)$_4$(OC$_6$H$_5$)$_4${μ-(CO)$_9$Co$_3$(μ_3-CCO$_2$)}$_4$·HOC$_6$H$_5$, 2c. A black column-like crystal was mounted on the top of a glass fiber, and data were collected on the CAD4 diffractometer. A difference map revealed that three of the tricobalt groups were disordered. The occupancies and displacement parameters of these atoms were refined with fractional site occupancies. All non-hydrogen atoms were refined with anisotropic thermal parameters, and hydrogen atoms were refined with a riding model and included in the final cycle, R1 = 0.0596 for 7753 reflections with $I > 2\sigma(I)$ and wR2(F^2) = 0.1729 for all data (1342 variables refined).

[Ti$_4$(μ_3-O)$_4$(2,6-(CH$_3$)$_2$-OC$_6$H$_3$)$_4${μ-(CO)$_9$Co$_3$(μ_3-CCO$_2$)}$_4$]·C$_6$H$_{14}$, 2d. A black column-like crystal was mounted on the top of a glass fiber, and data were collected on the CAD4 diffractometer. The molecular was found disordered on two sets of positions as if it rotated around its 2-fold axis for 90° so that every apex atom of a cubane-like core (alternating four Ti and four O atoms) was completely overlapped with a different type of atom from the other core, while the orientations of the two independent dimethylphenoxy groups of a set were different from those on the other set and were not overlapped. As for the two independent tricobalt cluster ligands, oxygen atoms from the carboxylato groups were completely disordered along with the cubane-like core and one of the two tricobalt units was also disordered. The cubane-like core was refined with 50% oxygen and 50% Ti. Refinement of the solvated hexane molecule with full occupancy yielded thermal parameters that were too high for carbon atoms, so in the final refinement the group occupancy was arbitrarily set to 0.5 and bond length restraint was applied. All hydrogen atoms were included in the refinement but restrained to ride on the atom to which they are bonded. The final refinement cycle converged to R1 = 0.1149 for 4299 reflections with $F_o{}^2 > 2\sigma(F_o{}^2)$ and wR2(F^2) = 0.3779 for all data (711 variables refined). Selected average distances and angles for **2a**−**d** are given in Table 4.

Ti$_6$(μ_3-O)$_4$(μ-OCH$_2$CH$_3$)$_4$(OCH$_2$CH$_3$)$_8${μ-(CO)$_9$Co$_3$(μ_3-CCO$_2$)}$_4$, 3. A black column-like crystal was mounted on the top of a glass fiber, and data were collected on the CAD4 diffractometer. A difference map revealed that three of the ethoxide groups and one of the tricobalt groups were disordered. The occupancies and displacement parameters of these atoms were refined with fractional site occupancies. All non-hydrogen atoms were refined with anisotropic thermal parameters in the final cycle, R1 = 0.0527 for 5286 unique reflections with $F_o{}^2 > 2\sigma(F_o{}^2)$ and wR2(F^2) = 0.1667 for all unique data, including those with negative intensities (697 variables refined). Selected distances and angles are given in Table 5.

[Ti$_6$(μ_3-O)$_2$(μ-O)$_2$(μ-OCH(CH$_3$)$_2$)$_2$(OCH(CH$_3$)$_2$)$_2$(1,2-O$_2$C$_6$H$_4$)$_4${μ-(CO)$_9$Co$_3$(μ_3-CCO$_2$)}$_4$], 4. The data diffraction data were collected on the FAST diffractometer. All hydrogen atoms were included in the refinement but restrained to ride on the atom to which they are bonded, and all non-hydrogen atoms were refined with anisotropic thermal parameters in the final cycles, R1 = 0.0489 for 10 160 reflections with $F_o{}^2 >$

Table 4. Selected Average Bond Lengths (Å) and Angles (deg) for 2a, 2b, 2c·HOC$_6$H$_5$, and 2d·C$_6$H$_{14}$[a]

	2a	**2b**	**2c**·HOC$_6$H$_5$	**2d**·C$_6$H$_{14}$
Ti···Ti	2.888(6)	2.896(2)	2.910(13)	2.79(6)
	3.039(9)	3.019(1)	3.021(8)	2.93(3)
Ti−μ_3-O	1.917(8)	1.912(4)	1.937(13)	1.986(5)
	2.104(3)	2.083(8)	2.102(11)	2.15(5)
Ti−O$_c$	2.040(6)	2.039(6)	2.03(2)	2.04(1)
Ti−OR	1.764(3)	1.748(3)	1.788(7)	1.81(1)
μ_3-O−Ti−μ_3-O	81.5(2)	81.2(3)	82.6(5)	90(2)
μ_3-O−Ti−OR	103(4)	103(3)	102(2)	97(1)
	172(1)	173(1)	173.5(5)	169(2)
μ_3-O−Ti−O$_c$	89(2)	89(2)	88.2(8)	86(2)
	161.6(9)	161.6(9)	162.9(5)	169(2)
	82(2)	82(2)	82.6(9)	80(2)
O$_c$−Ti−O$_c$	96.4(5)	96.7(2)	98(2)	96.4(7)
Ti−O−R	153.0(5)	144.9(9)−158.3(10)	145.4(8)−165.1(7)	169(3)
Ti−O$_c$−C	127(1)	127(1)	128.4(5)	126(2)
O$_c$−C−O$_c$	124.8(2)	124.9(5)	124.3(2)	126(2)
O$_c$−C−C	117.5(9)	117.6(7)	118(1)	117(1)

[a] O$_c$ = oxygen atom of carboxylate.

Table 5. Selected Bond Lengths (Å) and Angles (deg) for 3

Ti(1)−Ti(2)	3.114(2)	Ti(2)−O(11)	2.055(5)
Ti(1)−Ti(3)	2.983(2)	Ti(2)−O(31)	2.108(4)
Ti(2)−Ti(3)	3.106(2)	Ti(2)−O(41)	2.012(4)
Ti(3)−Ti(3′)	3.169(2)	Ti(2)−O(61)	1.768(5)
Ti(1)−O(1)	1.995(4)	Ti(2)−O(71)	1.800(5)
Ti(1)−O(2)	1.866(4)	Ti(3)−O(1)	1.891(4)
Ti(1)−O(12)	2.105(4)	Ti(3)−O(2)	2.106(4)
Ti(1)−O(22)	2.057(5)	Ti(3)−O(2′)	1.921(4)
Ti(1)−O(31)	1.927(4)	Ti(3)−O(21)	2.111(4)
Ti(1)−O(51)	1.754(5)	Ti(3)−O(41)	1.994(4)
Ti(2)−O(1)	1.999(4)	Ti(3)−O(81)	1.772(4)
O(1)−Ti(1)−O(2)	82.7(2)	O(1)−Ti(3)−O(21)	85.1(2)
O(1)−Ti(1)−O(12)	85.1(2)	O(1)−Ti(3)−O(41)	77.5(2)
O(1)−Ti(1)−O(22)	82.3(2)	O(1)−Ti(3)−O(81)	106.8(2)
O(1)−Ti(1)−O(31)	79.9(2)	Ti(1)−O(1)−Ti(2)	102.4(2)
O(1)−Ti(1)−O(51)	175.5(2)	Ti(1)−O(1)−Ti(3)	100.3(2)
O(1)−Ti(2)−O(11)	86.9(2)	Ti(2)−O(1)−Ti(3)	105.9(2)
O(1)−Ti(1)−O(31)	75.6(2)	Ti(1)−O(2)−Ti(3)	97.2(2)
O(1)−Ti(2)−O(41)	74.7(2)	Ti(1)−O(2)−Ti(3′)	158.6(2)
O(1)−Ti(2)−O(61)	97.8(2)	Ti(3′)−O(2)−Ti(3)	103.7(2)
O(1)−Ti(2)−O(71)	162.4(2)	Ti(1)−O(31)−Ti(2)	100.9(2)
O(1)−Ti(3)−O(2)	79.2(2)	Ti(2)−O(41)−Ti(3)	101.7(2)
O(1)−Ti(3)−O(2′)	153.4(2)		

Table 6. Bond Lengths (Å) and Angles (deg) for 4

Ti(1)−Ti(3)	3.0494(10)	Ti(2)−O(42)	1.936(3)
Ti(1)−Ti(2)	3.1331(10)	Ti(2)−O(1)	2.010(2)
Ti(2)−Ti(3)	3.1409(11)	Ti(2)−O(21)	2.032(3)
Ti(1)−O(2)	1.794(2)	Ti(2)−O(12)	2.040(2)
Ti(1)−O(41)	1.873(3)	Ti(3)−O(2′)	1.806(2)
Ti(1)−O(1)	1.919(2)	Ti(3)−O(32)	1.868(3)
Ti(1)−O(51)	1.995(2)	Ti(3)−O(1)	1.939(2)
Ti(1)−O(11)	2.039(2)	Ti(3)−O(51)	1.971(3)
Ti(1)−O(42)	2.178(2)	Ti(3)−O(22)	2.033(3)
Ti(2)−O(61)	1.760(2)	Ti(3)−O(31)	2.188(2)
Ti(2)−O(31)	1.931(3)	O(2)−Ti(3′)	1.806(2)
O(2)−Ti(1)−O(1)	107.11(11)	O(1)−Ti(3)−O(51)	77.00(10)
O(41)−Ti(1)−O(1)	150.96(11)	O(1)−Ti(3)−O(22)	83.11(10)
O(1)−Ti(1)−O(51)	76.89(10)	O(1)−Ti(3)−O(31)	75.01(9)
O(1)−Ti(1)−O(11)	85.80(10)	Ti(1)−O(1)−Ti(3)	104.47(11)
O(1)−Ti(1)−O(42)	75.13(9)	Ti(1)−O(1)−Ti(2)	105.77(11)
O(61)−Ti(2)−O(1)	178.59(11)	Ti(3)−O(1)−Ti(2)	105.38(11)
O(31)−Ti(2)−O(1)	79.48(10)	Ti(1)−O(2)−Ti(3′)	158.5(2)
O(42)−Ti(2)−O(1)	78.84(10)	Ti(2)−O(31)−Ti(3)	99.17(10)
O(1)−Ti(2)−O(21)	84.21(10)	Ti(2)−O(31)−Ti(3)	99.17(10)
O(1)−Ti(2)−O(12)	85.26(10)	Ti(2)−O(42)−Ti(1)	99.03(10)
O(2′)−Ti(3)−O(1)	107.92(11)	Ti(3)−O(51)−Ti(1)	100.53(11)
O(32)−Ti(3)−O(1)	151.34(11)		

Table 7. Selected Bond Lengths (Å) and Angles (deg) for 5

Co(1)−Ti(1)	3.0276(14)	Co(1)−O(31)	2.152(4)
Co(1)−Ti(1A)	3.0311(14)	Ti(1)−O(41)	1.756(4)
Co(1)−O(33)	2.030(4)	Ti(1)−O(32)	1.931(4)
Co(1)−O(32)	2.033(4)	Ti(1)−O(33A)	1.934(4)
Co(1)−O(21)	2.051(4)	Ti(1)−O(12A)	2.034(4)
Co(1)−O(11)	2.065(4)	Ti(1)−O(22)	2.043(4)
Co(1)−O(31A)	2.130(4)	Ti(1)−O(31)	2.053(4)
O(33)−Co(1)−O(11)	86.0(2)	O(41)−Ti(1)−O(32)	99.2(2)
O(33)−Co(1)−O(31A)	81.2(2)	O(32)−Ti(1)−O(12A)	165.8(2)
O(33)−Co(1)−O(31)	85.1(2)	Ti(1)−O(31)−Co(1A)	92.9(2)
O(33)−Co(1)−O(21)	104.5(2)	Ti(1)−O(31)−Co(1)	92.1(2)
O(33)−Co(1)−O(32)	162.2(2)	Co(1A)−O(31)−Co(1)	99.4(2)
O(32)−Ti(1)−O(33A)	86.1(2)	Ti(1)−O(32)−Co(1)	99.6(2)
O(32)−Ti(1)−O(22)	85.4(2)	Ti(1A)−O(33)−Co(1)	99.7(2)
O(32)−Ti(1)−O(31)	86.3(2)		

$2\sigma(F_o^2)$ and wR2(F^2) = 0.1051 for all data (712 variables refined). Selected distances and angles are given in Table 6.

[Ti$_2$Co$_2${(OCH$_2$)$_3$CCH$_3$}$_2$(OCH(CH$_3$)$_2$)$_2${μ-(CO)$_9$Co$_3$(μ_3-CCO$_2$)}$_4$], 5. A black column-like crystal was mounted on the top of a glass fiber, and data were collected on the CAD4 diffractometer. A difference map revealed that three of the tricobalt groups were disordered. The occupancies and displacement parameters of these atoms were refined with fractional site occupancies. All non-hydrogen atoms were refined with anisotropic thermal parameters, and hydrogen atoms were refined with a riding model and included in the final cycle, R1 = 0.0515 for 4880 reflections with $F_o^2 > 2\sigma(F_o^2)$ and wR2(F^2) = 0.1493 for 6613 reflections measured (577 variables refined). Selected distances and angles are given in Table 7.

[{Co$_3$Ti(OCH$_3$)$_6$(HOCH$_3$)(THF){μ-(CO)$_9$Co$_3$(μ_3-CCO$_2$)}$_3$}$_2$-(O$_2$CCO$_2$)]·2HOCH$_3$·2THF, 6. A red-brown platelike crystal was mounted on the top of a glass fiber, and data were collected on the FAST diffractometer. All non-hydrogen atoms were refined with anisotropic thermal parameters, and hydrogen atoms were refined with isotropic thermal parameters in the final cycle, R1 = 0.0843 for 9073 observed unique reflections with $I > 2\sigma(I)$ and wR2(F^2) = 0.2159 for 18 826 reflections measured (977 variables refined). Selected distances and angles are given in Table 8.

Results and Discussion

Solid State Structures. The principal characterization of the new compounds was by means of single-crystal X-ray diffraction, and the structural information obtained is presented in order of increasing nuclearity of the M(IV) core. In all cases, the bond distances and angles of the tricobalt cluster substituents are unchanged from those of the free ligand within experimental error.[41] Bond distances and angles associated with the M(IV) core are intercompared in the Support-

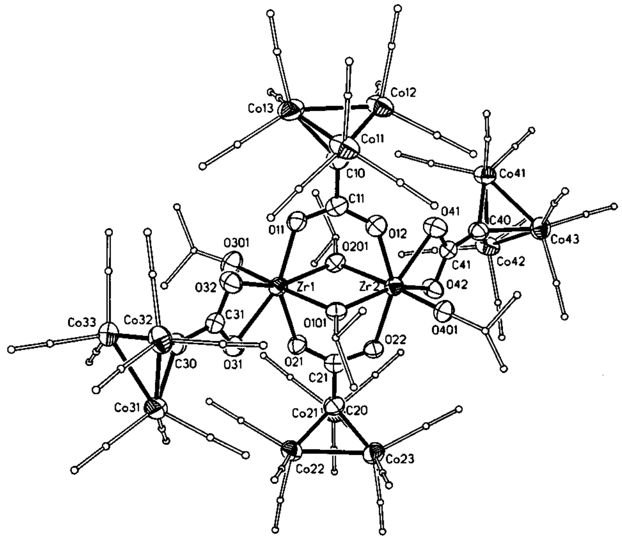

Figure 1. ORTEP diagram of $Zr_2(\mu\text{-}OCH(CH_3)_2)_2(OCH(CH_3)_2)_2\{\mu\text{-}(CO)_9Co_3(\mu_3\text{-}CCO_2)\}_2\{(CO)_9Co_3(\mu_3\text{-}CCO_2)\}_2$, **1**, with thermal ellipsoids at 40% probability. The radii of the carbon and oxygen atoms of the CO groups and the carbon atoms of the isopropoxy ligands are set at arbitrary values for clarity.

Table 8. Selected Bond Lengths (Å) and Angles (deg) for 6·2HOCH$_3$·2THF

Co(1)−Ti	3.155(2)	Co(2)−O(42)	2.057(6)
Co(2)−Co(3)	2.977(2)	Co(3)−O(1)	2.119(7)
Co(1)−O(1)	2.024(6)	Co(3)−O(3)	2.101(6)
Co(1)−O(2)	2.146(6)	Co(3)−O(4)	2.159(6)
Co(1)−O(3)	2.132(7)	Co(3)−O(6)	2.118(7)
Co(1)−O(11)	2.056(6)	Co(3)−O(12)	2.021(7)
Co(1)−O(5)	2.086(8)	Co(3)−O(31)	2.016(6)
Co(1)−O(21)	2.056(6)	Ti−O(2)	2.101(7)
Co(2)−O(1)	2.026(6)	Ti−O(3)	2.065(7)
Co(2)−O(2)	2.120(6)	Ti−O(4)	2.011(6)
Co(2)−O(4)	2.137(6)	Ti−O(7)	1.761(7)
Co(2)−O(32)	2.055(6)	Ti−O(8)	1.813(7)
Co(2)−O(41)	2.122(7)	Ti−O(22)	2.018(6)
O(1)−Co(1)−O(11)	89.5(3)	O(7)−Ti−O(22)	99.1(3)
O(1)−Co(1)−O(3)	87.8(3)	O(7)−Ti−O(2)	92.5(3)
O(1)−Co(1)−O(2)	78.4(2)	O(7)−Ti−O(3)	173.6(3)
O(1)−Co(1)−O(5)	95.4(3)	Co(1)−O(1)−Co(2)	104.9(3)
O(1)−Co(1)−O(21)	167.6(3)	Co(1)−O(1)−Co(3)	92.8(3)
O(1)−Co(2)−O(32)	91.1(3)	Co(2)−O(1)−Co(3)	91.8(3)
O(1)−Co(2)−O(2)	79.0(2)	C(2)−O(2)−Ti	121.7(6)
O(1)−Co(2)−O(41)	94.9(3)	Ti−O(2)−Co(2)	100.2(3)
O(1)−Co(2)−O(4)	88.9(3)	Ti−O(2)−Co(1)	95.9(2)
O(1)−Co(2)−O(42)	172.3(3)	Co(2)−O(2)−Co(1)	97.7(2)
O(31)−Co(3)−O(1)	89.4(2)	Ti−O(3)−Co(3)	104.6(3)
O(12)−Co(3)−O(1)	88.5(3)	Ti−O(3)−Co(1)	97.5(3)
O(3)−Co(3)−O(1)	86.2(2)	Co(3)−O(3)−Co(1)	90.3(2)
O(1)−Co(3)−O(4)	86.0(2)	Ti−O(4)−Co(2)	102.6(3)
O(1)−Co(3)−O(6)	175.6(3)	Ti−O(4)−Co(3)	104.4(3)
O(7)−Ti−O(8)	95.9(4)	Co(2)−O(4)−Co(3)	87.7(2)
O(7)−Ti−O(4)	97.3(3)	C(5)−O(5)−Co(1)	126.2(9)

ing Information, and only selected structural parameters are highlighted in the following discussion.

$Zr_2(\mu\text{-}OCH(CH_3)_2)_2(OCH(CH_3)_2)_2\{\mu\text{-}(CO)_9Co_3(\mu_3\text{-}CCO_2)\}_2\{(CO)_9Co_3(\mu_3\text{-}CCO_2)\}_2$, 1. A single-crystal X-ray diffraction study shows that in the solid state there are two independent molecules of **1** in an asymmetric unit. Both molecules have similar structures (Figure 1) but differ in the orientation of the tricobalt clusters and in the conformation of the isopropoxy groups. Symmetrical bridging and chelating cluster ligands are observed, in agreement with the IR results.

The coordination sphere of a single zirconium atom of **1** can be described as a slightly distorted pentagonal bipyramid in which the five equatorial positions are occupied with two oxygen atoms from a chelating cluster ligand, two from bridging cluster ligands, and one from a bridging isopropoxy group (sum of O−Zr−O angles is 357.9(3)°). The apical positions are occupied with oxygen atoms from one terminal and one bridging isopropoxy group (average O−Zr−O angle = 174.8(7)°). The Zr−O distances for bridging isopropoxy groups (average 2.154(9) Å) are considerably longer than the Zr−O distances for terminal groups (average 1.895(2) Å). The terminal isopropoxy groups are linearly coordinated to Zr (average Zr−O−C angle = 172.6(14)°), facilitating strong O → Zr π-donation. The Zr−O distances for the bridging cluster ligands (average 2.189(8) Å) are shorter than those of the chelating cluster carboxylates (2.260(5) Å).

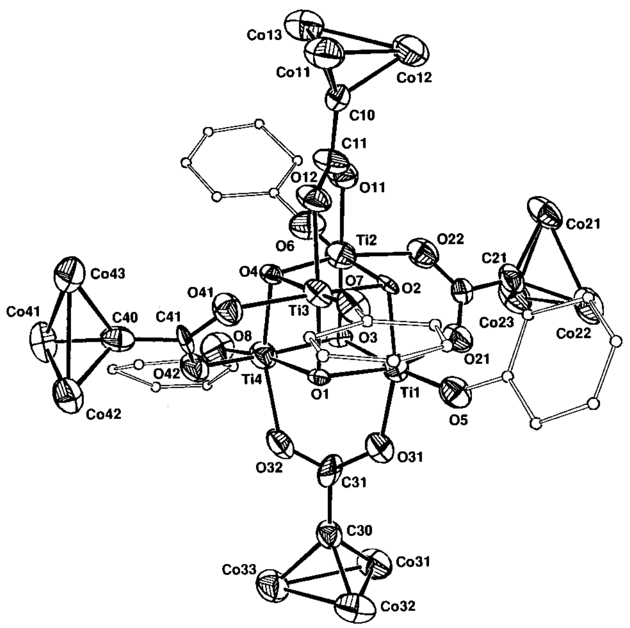

Figure 2. The structure of $[Ti_4(\mu_3\text{-}O)_4(OC_6H_5)_4\{\mu\text{-}(CO)_9Co_3(\mu_3\text{-}CCO_2)\}_4]$, **2c**, with thermal ellipsoids at 40% probability. The carbon atoms of the phenoxy ligands are set at arbitrary values and the CO groups are omitted for clarity.

Compound **1** is the first example of a structurally characterized zirconium alkoxy carboxylate. The Zr−Zr separation in **1** (3.3496(8) Å) is significantly shorter than those of $[Zr(OCH(CH_3)_2)_4\cdot HOCH(CH_3)_2]_2$,[45] $[\{H_3CC(CH_2O)_3\}_2Zr_4(OCH(CH_3)_2)_{12}]$,[46] heteroleptic zirconium alkoxides (3.48−3.51 Å),[47−49] and $Zr_4O_2(O_2CCH(CH_3)_2)_{12}$ (3.59−3.74 Å).[37] This may be due to the bite size of the cluster carboxylate.

$Ti_4(\mu_3\text{-}O)_4(OR)_4\{\mu\text{-}(CO)_9Co_3(\mu_3\text{-}CCO_2)\}_4$, 2. Single-crystal X-ray structural analyses show that compounds **2** all have similar structures. The structure of **2c** is shown in Figure 2 as a representative example. The core is a distorted Ti_4O_4 cube with titanium and oxo

---

(45) Vaartstra, B. A.; Huffman, J. C.; Gradeff, P. S.; Huber-Pfalzgraf, L. G.; Daran, J.; Parraud, S.; Yunlu, K.; Caulton, K. G. *Inorg. Chem.* **1990**, *29*, 3126.

(46) Boyle, T. J.; Schwartz, R. W.; Doedens, R. J.; Ziller, J. W. *Inorg. Chem.* **1995**, *34*, 1110.

(47) Samuels, J. A.; Vaartstra, B. A.; Huffman, J. C.; Trojan, K. L.; Hatfield, W. E.; Caulton, K. G. *J. Am. Chem. Soc.* **1990**, *112*, 9623.

(48) Sogani, S.; Singh, A.; Bohra, R.; Mehrotra, R. C.; Nottemeyer, M. *J. Chem. Soc., Chem. Commun.* **1991**, 738.

(49) Schmid, R.; Mosset, A.; Galy, J. *Inorg. Chim. Acta* **1991**, *179*, 167.

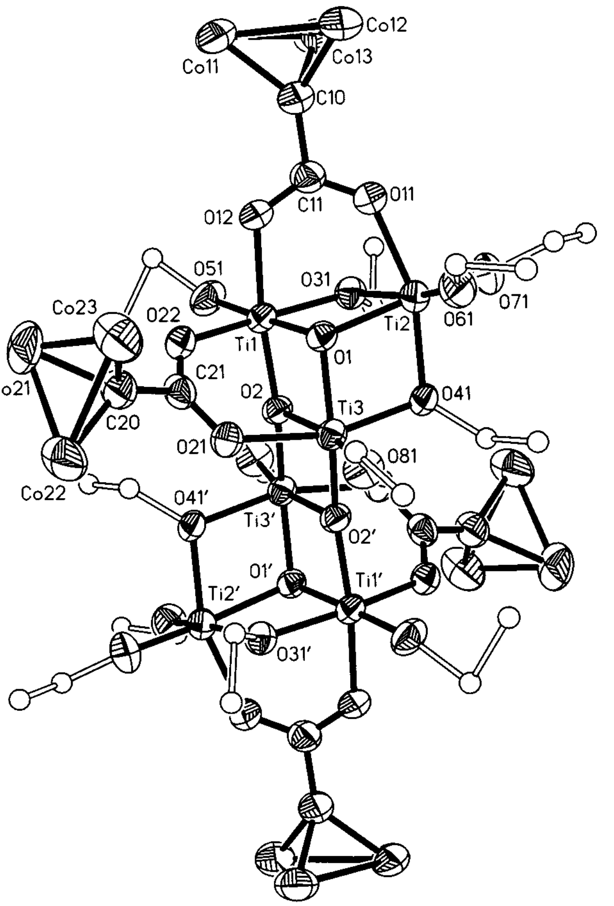

Figure 3. The molecular structure of $Ti_6(\mu_3\text{-}O)_4(\mu\text{-}OCH_2CH_3)_4(OCH_2CH_3)_8\{\mu\text{-}(CO)_9Co_3(\mu_3\text{-}CCO_2)\}_4$, **3**, with thermal ellipsoids at 40% probability. The CO groups are omitted for clarity.

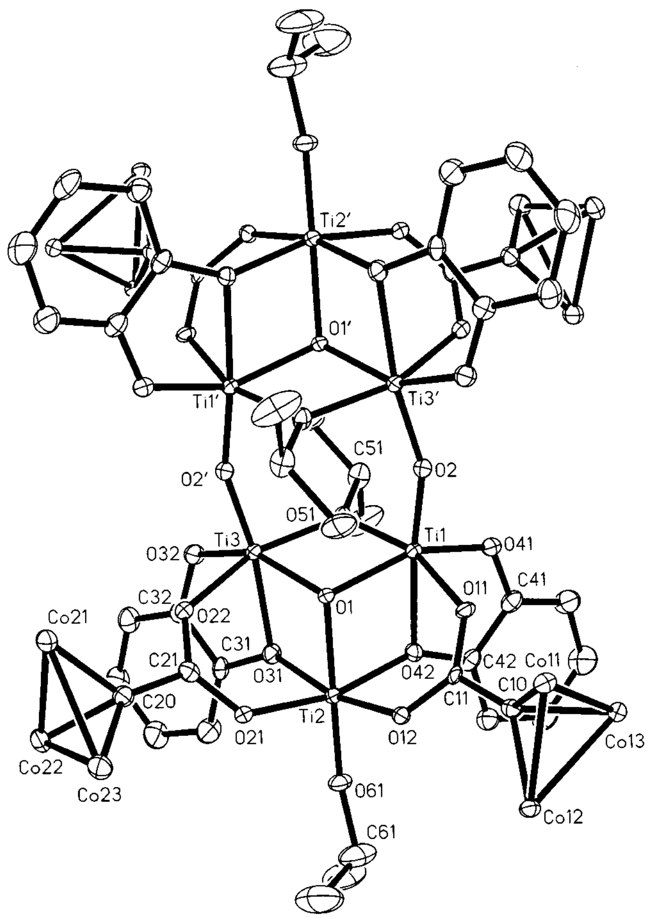

Figure 4. ORTEP diagram of $[Ti_6(\mu_3\text{-}O)_2(\mu\text{-}O)_2(\mu\text{-}OCH(CH_3)_2)_2(OCH(CH_3)_2)_2(1,2\text{-}O_2C_6H_4)_4\{\mu\text{-}(CO)_9Co_3(\mu_3\text{-}CCO_2\}_4]$, **4**, with thermal ellipsoids at 50% probability. The CO groups are omitted for clarity.

oxygen atoms occupying alternative vertices. Molecules **2a**, **2b**, and **2d** lie on crystallographic C_2 axes, while **2c** is in a general position. All have virtual S_4 symmetry. The coordination sphere of each Ti atom is a distorted octahedron of oxygen atoms: three derived from bridging oxo ligands, two from bridging cluster ligands, and one from a terminal alkoxy or aryloxy ligand. The cluster carboxylates bridge four of the six edges of the Ti_4 tetrahedron, and the four bridged edges form a butterfly shape such that a C_2 axis runs through the centers of the two unbridged edges. Thus, the four tricobalt clusters lie roughly in a plane perpendicular to the C_2 axis with one transoid pair being displaced slightly up and one pair down. The R groups of the alkoxy or aryloxy ligands project above and below the plane of the tricobalt clusters. There is considerable open space in the structure, but this decreases with increasing size of the R group.

$Ti_6(\mu_3\text{-}O)_4(\mu\text{-}OCH_2CH_3)_4(OCH_2CH_3)_8\{\mu\text{-}(CO)_9Co_3(\mu_3\text{-}CCO_2)\}_4$, 3. The solid state structure reveals that **3** is a dimer of two identical units (Figure 3). Each of these units contains a Ti_3O_4 core fragment which can be derived from the Ti_4O_4 cube in **2** by removing one Ti vertex. The units are linked by TiO edges oriented so that the Ti_3O_4 units are related to each other by a crystallographic inversion center of symmetry. Consequently, there are two types of μ_3-O ligands, planar and pyramidal, with the former constituting the interfragment connections. Each Ti_3O_4 unit is bridged by two cluster ligands, and the remaining coordination sites are occupied by six ethoxy ligands, two of which are bridging. As with **2**, the coordination environment of a Ti atom is a distorted octahedron; however, there are three different environments: Ti(1), oxygen atoms from two cluster carboxylates, two μ_3-oxo ligands, one bridging ethoxy, and one terminal ethoxy; Ti(2), oxygen atoms from one cluster carboxylate, one μ_3-oxo ligand, two bridging ethoxys, and two terminal ethoxys; Ti(3), oxygen atoms from one cluster carboxylate, three μ_3-oxo ligands, one bridging ethoxy, and one terminal ethoxy.

$Ti_6(\mu_3\text{-}O)_2(\mu\text{-}O)_2(\mu\text{-}OCH(CH_3)_2)_2(OCH(CH_3)_2)_2(1,2\text{-}O_2C_6H_4)_2)_4\{\mu\text{-}(CO)_9Co_3(\mu_3\text{-}CCO_2)\}_4$, 4. A single-crystal X-ray structural analysis shows that in the solid state **4** is, like **3**, a dimer of two identical units related by an inversion center of symmetry (Figure 4). The coordination environments of the Ti centers are near octahedral, and similar to the structure of **3**, there are three different sites: Ti(1), oxygen atoms from one cluster carboxylate, one μ_3-oxo, one μ_2-oxo, one bridging isopropoxy, and one bridging and one terminal oxygen from one catechol; Ti(2), oxygen atoms from two cluster carboxylates, one μ_3-oxo, one terminal isopropoxy, and two bridging oxygens from two catechols; and Ti(3), oxygen atoms from one cluster carboxylate, one μ_3-oxo, one μ_2-oxo, one bridging isopropoxy, one terminal isopropoxy, and one bridging and one terminal oxygen from one catechol. An interesting feature is the catechol ligand which uses one oxygen to bridge two Ti centers

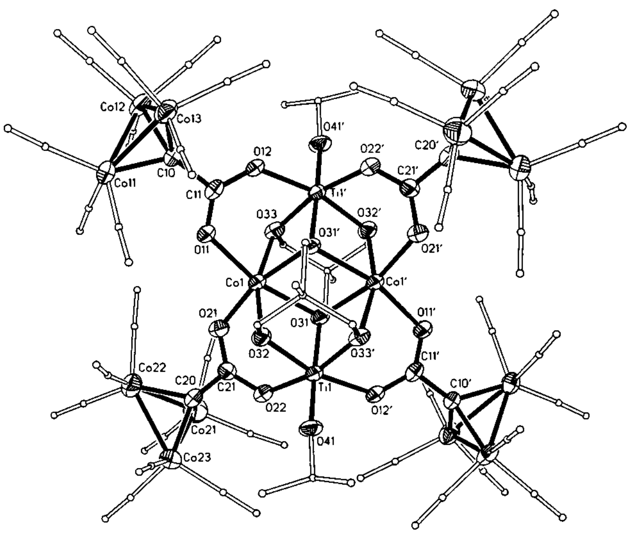

Figure 5. ORTEP diagram of $[Ti_2Co_2\{(\mu_3\text{-}OCH_2)(\mu\text{-}OCH_2)_2\text{-}CCH_3\}_2(OCH(CH_3)_2)_2\{\mu\text{-}(CO)_9Co_3(\mu_3\text{-}CCO_2)\}_4]$, **5**, with thermal ellipsoids at 40% probability. The radii of the carbon and oxygen atoms of the CO groups and the carbon atoms of the isopropoxy and tris(hydroxymethyl)ethane ligands are set at arbitrary values for clarity.

and the other to coordinate to one of the two Ti atoms in a terminal fashion.

$[Co_2Ti_2(OCH_2)_3CCH_3)_2(OCH(CH_3)_2)_2\{\mu\text{-}(CO)_9Co_3\text{-}(\mu_3\text{-}CCO_2)\}_4]$, 5. The solid state structure of **5** is shown in Figure 5. Similar to the structures **3** and **4**, the core of **5** contains two M_3O_4 incomplete cubes related by a crystallographic inversion center. However, the two partial cubes have the heteronuclear composition, Co_2TiO_4 and share a Co_2O_2 face such that the line connecting the Co atoms constitutes a C_2 axis, thereby placing the openings of the cubes transoid to each other. These openings are capped by the organic fragments of the tridentate ligand $(OCH_2)_3CCH_3$. The molecular symmetry is C_{2h}. The coordination sphere of both the Ti and Co centers are distorted octahedra, and the six oxygen atoms originate as follows: Ti(1), two from cluster carboxylates (each from different carboxylate), two μ-O and one μ_3-O from the tridentate ligands (two from one and one from another), and one terminal isopropoxy; Co(1), two from cluster carboxylates (each from a different carboxylate), and two μ-O and two μ_3-O from the tridentate ligands (two from one and two from another).

Heteronuclear titanium alkoxides or oxoalkoxides are known, e.g., $\{[(C_8H_{12})Rh]_2[Ti(O(CH_2)_2CH_3)_6]\}$,[50] $Ba_4Ti_{13}O_{18}(OCH_2CH_2OCH_3)_{24}$;[51] however, heteronuclear titanium alkoxy carboxylates are rare. The only crystallographically characterized compound is $Pb_2Ti_4(\mu_4\text{-}O)(CH_3CO_2)_2(\mu_3\text{-}OCH_2CH_3)_8(OCH_2CH_3)_6$.[52] Compound **5** is the first cobalt–titanium alkoxy carboxylate to be structurally characterized, and a couple of the structural parameters merit comment. The Ti–μ_3-O distance (2.053(4) Å) is significantly shorter than that in known titanium alkoxides and even oxoalkoxides, e.g. $[Ti_4(\mu_3\text{-}OCH_2CH_3)_2(\mu\text{-}OCH_2CH_3)_6(OCH_2CH_3)_8$ (2.15–2.23 Å),[53] $[(H_3CC(CH_2\text{-}\mu_3\text{-}O)(CH_2\text{-}\mu\text{-}O)_2Ti_4(OCH(CH_3)_2)_{10}]$ (2.20 Å),[46] and $[Ti_3(\mu_3\text{-}O)(\mu_3\text{-}OCH_3)(\mu\text{-}OCH(CH_3)_2)_3(OCH(CH_3)_2)_6$ (2.18 Å).[27] On the other hand, Co–O distances range from 2.030 to 2.152 Å, among which the longest distance involves the interaction between the Co atom and the μ_3-O of the tridentate ligand.

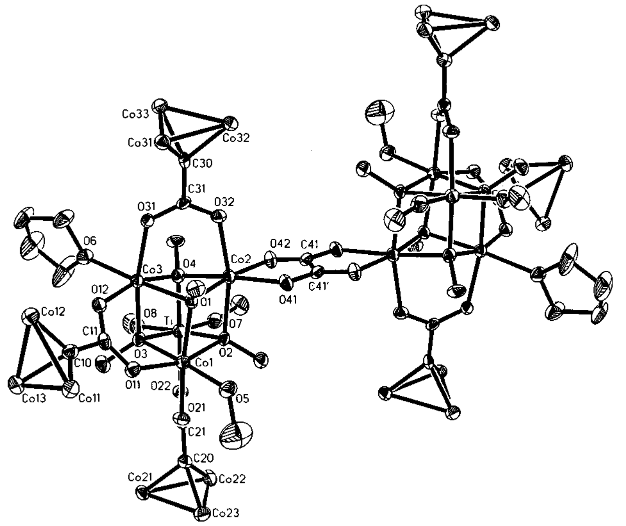

Figure 6. ORTEP diagram of $[\{Co_3Ti(\mu_3\text{-}OCH_3)_4(OCH_3)_2\text{-}(HOCH_3)(THF)\{\mu\text{-}CO)_9Co_3(\mu_3\text{-}CCO_2)\}_3\}_2(O_2CCO_2)]$, **6**, with thermal ellipsoids at 40% probability. The CO groups are omitted for clarity.

$[\{Co_3Ti(OCH_3)_6(HOCH_3)(THF)\{\mu\text{-}(CO)_9Co_3(\mu_3\text{-}CCO_2)\}_3\}_2(O_2CCO_2)]$, 6. A single-crystal diffraction study of **6** reveals the rather unusual double cube structure shown in Figure 6. Two complete $Co_3Ti(OCH_3)_4$ cubes, related by a center of symmetry, are joined by a bridging tetradentate oxalate ligand. Each cube has a mixed-metal core structure similar to that of **2** with one cluster carboxylate removed. The coordination environments of both the Ti and Co centers are near octahedral with six oxygen atoms derived as follows: Ti, one from cluster carboxylate, three μ_3-OCH_3, and two terminal $-OCH_3$; Co(1), two from cluster carboxylate, three μ_3-OCH_3, and one terminal $HOCH_3$; Co(2), one from cluster carboxylate, three μ_3-OCH_3, and two oxalate ligand; Co(3), two from cluster carboxylate, three μ_3-OCH_3, and one THF. On a single cube, the three tricobalt clusters lie in an approximate plane, but the cluster planes of each cube are displaced with respect to each other. There are now large empty spaces between the two cubes.

An alternative way to describe the core structures of compounds **1**–**6** is to use the coordination polyhedra shown in Chart 1 in which the curved line represents the position of the cluster carboxylate ligand. This common representation of group 4 metal oxides shows the inter-relationships between the new compounds and related organic derivatives. Thus, the complete Zr_2O_{12} core structure (Chart 1a) of **1** is represented as two pentagonal bypyramids each sharing one nonequatorial edge. The Ti_4O_{16} core (Chart 1b) in **2** consists of four TiO_6 octahedra sharing one face each. This is a variant of the structure observed for $[Ti(OEt)_4]_4$[54] shown in Chart 1c but very different from that of **1**. There is one previous report of an cubane-like structure derived from

---

[50] Day, V. W.; Eberspacher, T. A.; Hao, J.; Klemperer, W. G.; Zhong, B. *Inorg. Chem.* **1995**, *34*, 3549.

[51] Campion, J.-F.; Payne, D. A.; Chae, H. K.; Maurin, J. K.; Wilson, S. R. *Inorg. Chem* **1991**, *30*, 3244.

[52] Daniele, S.; Papiernick, R.; Hubert-Pfalztraf, L. G.; Jagner, S.; Hakansson, M. *Inorg. Chem.* **1995**, *34*, 628.

[53] Ibers, J. A. *Nature* **1963**, *197*, 686.

[54] Bradley, D. C.; Mehrotra, R. C.; Gaur, D. P. *Metal Alkoxides*; Academic Press: London, 1978.

Chart 1

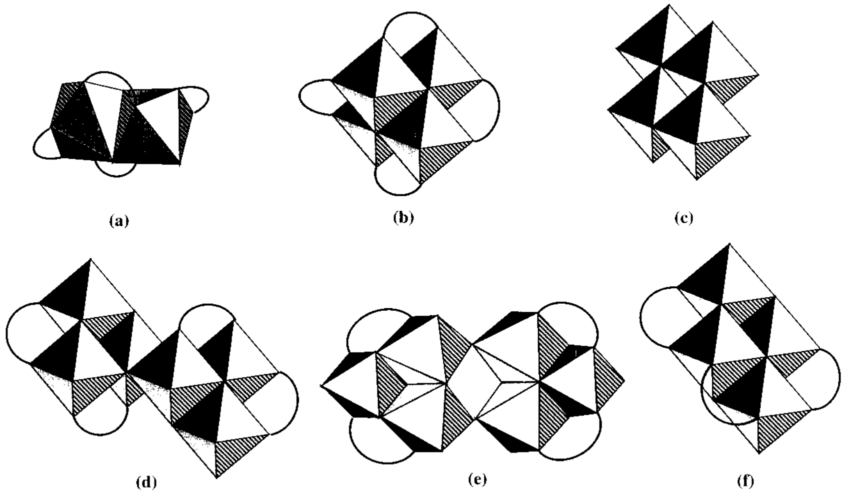

an organic acid, i.e., $Ti_4(\mu_3\text{-}O)_4(\mu\text{-}(CH_3)_2CHCO_2)_4(OC(CH_3)_3)_4$.[55] The geometric representation of the core structure in **3**, shown in Chart 1d, suggests a close relationship with compounds **2**. Each of the identical trimer units of **3** contains a $[TiO_4]_3$ unit derived from the $[TiO_4]_4$ structures (Chart 1b,c) by removal of one face-sharing octahedral TiO_4 fragment. The structure of **3** consists of edge-sharing $[TiO_4]_3$ units arranged to produce a center of inversion. As with **2**, the four tricobalt clusters roughly lie in a plane with the ethoxy ligands above and below the plane. Whereas the arrangement of the cobalt clusters in **2** is nearly square planar, that in **3** is elongated in the direction of the ladder-like Ti_6 core. A hexanuclear titanium oxoalkoxycarboxylate, derived from an organic acid and having the same core structure as **3**, $Ti_6(\mu_3\text{-}O_4)(\mu\text{-}OCH(CH_3)_2)_4(OCH(CH_3)_2)_8(\mu\text{-}(CH_3)_3CCH_2CO_2)_4$, has been recently reported.[56,57] The simplicity of the structural relationship between **3** and **4** is better revealed by a comparison of the representations in Chart 1d,e. Compound **4** contains the same $[TiO_4]_3$ units as **3** except that they are now joined by vertex so that a center of inversion is generated. The disposition of the tricobalt clusters and alkoxy ligands remains similar to that of **3**. Indeed, the core structure of **4** is that of the known $Ti_6(\mu_3\text{-}O)_2(\mu\text{-}O)_2(\mu\text{-}OCH(CH_3)_2)_6(OCH(CH_3)_2)_6\{\mu\text{-}CH_3CO_2\}_4$ which is derived from an organic acid.[33,34] In terms of fused octahedra, **5** represents another variation on the structural theme of **2** and $[Ti(OEt)_4]_4$ (Chart 1b,c), i.e., the position of the fourth $[MO_4]$ octahedron relative to the triangular $[MO_4]_3$ fragment is different (Chart 1f). Once again, the four tricobalt clusters roughly lie in a plane with the alkoxy ligands projecting above and below it. As with **2** and **3**, a rectangular array of clusters results albeit intermediate in the longer dimension.

Syntheses. All compounds were prepared by the reaction of the cluster acid with the appropriate metal alkoxides. Simple crystallization permits the single cluster M(IV) alkoxycarboxylate formed to be isolated in good yield.

$Zr_2(\mu\text{-}OCH(CH_3)_2)_2(OCH(CH_3)_2)_2\{\mu\text{-}(CO)_9Co_3(\mu_3\text{-}CCO_2)\}_2\{(CO)_9Co_3(\mu_3\text{-}CCO_2)\}_2$, 1. The 4:1 stoichiometric reaction of $(CO)_9Co_3(\mu_3\text{-}CCO_2H)$ and $[Zr(OCH(CH_3))_4{\cdot}HOCH(CH_3)_2]_2$ in THF gave a crystalline product in high yield upon removal of the solvent. The solid state infrared spectrum exhibits bands characteristic of the carbonyl ligands of the cluster substituent, bridging carboxylates, chelating carboxylates, as well as alkoxide groups.[58,54] The ^1H NMR spectrum shows only a single type of isopropyl group, suggesting a fluxional species in solution, since the isopropyl alcohol adduct of zirconium(IV) isopropoxide has a dinuclear structure in which each zirconium is octahedrally coordinated by three terminal and two bridging isopropoxy groups and one terminal isopropyl alcohol molecule.[58] The reaction of $[Zr(OCH(CH_3)_2)_4{\cdot}HOCH(CH_3)_2]_2$ and $(CO)_9Co_3(\mu_3\text{-}CCO_2H)$ seems straightforward, i.e. four isopropoxy groups are replaced by four cluster substituted ligands.

$$4(CO)_9Co_3(\mu_3\text{-}CCO_2H) + [Zr(OCH(CH_3)_2)_4{\cdot}HOCH(CH_3)_2]_2 \rightarrow \mathbf{1} + 6HOCH(CH_3)_2$$

$Ti_4(\mu_3\text{-}O)_4(OR)_4\{\mu\text{-}(CO)_9Co_3(\mu_3\text{-}CCO_2)\}_4$, 2. These compounds were prepared from $Ti(OR)_4$ (**2a**, R = R = $CH(CH_3)_2$; **2b**, R = $(CH_2)_3CH_3$) and $Ti(CH(CH_3)_2)_3(OR)$ (**2c**, R = C_6H_5; **2d**, R = 2,6-$(CH_3)_2$-C_6H_3)). For the last two compounds, only the aryl groups are found in the isolated products. In each case, the solid state infrared spectrum exhibits bands characteristic of the carbonyl ligands of the cluster substituent, bridging carboxylates, and alkoxide groups. The ^1H and ^{13}C NMR spectra show only one kind of alkyl or aryl group for each compound. In the case of M = Ti and R = $CH(CH_3)_2$, an increase of the cluster acid:alkoxide ratio by a factor of two had no observed effect on the reaction path or yield. In this case, the excess cluster acid was isolated after reaction. The cluster ester $(CO)_9Co_3(\mu\text{-}CC(O)OCH(CH_3)_2)$, a known stable compound with a characteristic spectroscopic signature, was never observed as a coproduct. On the other hand, $(CH_3)_2CHOH$ and $\{(CH_3)_2CH\}_2O$ were observed by IR in the volatiles removed from the reaction mixture. The latter was identified by

---

(55) Charnick, S. G.; Day, V. W.; Klemperer, W. J. Personal communication.

(56) Boyle, T. J.; Tafoya, C. J.; Scott, B. *Abstracts of Papers*, 211th National Meeting of the American Chemical Society, New Orleans, LA, Spring 1996; American Chemical Society: Washington, DC, 1996; abstract O62.

(57) Boyle, T. J. Personal communication.

(58) Mehrotra, R. C.; Bohra, R. *Metal Carboxylates*; Academic Press: New York, 1983; pp 396.

two bands in the difference spectrum that clearly distinguish it from the alcohol, i.e., 1368 and 1167 cm^{-1}. Monitoring the reaction by IR spectroscopy also showed that $(CO)_9Co_3(\mu\text{-}CCO_2H)$ reacts rapidly with $Ti(OR)_4$ (<5 min), as indicated by the loss of the characteristic bands for the carboxylic acid group and formation of metal carboxylate bands, albeit not those of the final product. Thus, the proposed reaction for the formation of compounds **2** is as follows:

$$4(CO)_9Co_3(\mu_3\text{-}CCO_2H) + 4Ti(OR)_4 \rightarrow \mathbf{2} + 4ROH + 4ROR$$

$Ti_6(\mu_3\text{-}O)_4(\mu\text{-}OCH_2CH_3)_4(OCH_2CH_3)_8\{\mu\text{-}(CO)_9Co_3\text{-}(\mu_3\text{-}CCO_2)\}_4$, 3. The reaction of $Ti(OCH_2CH_3)_4$ and $(CO)_9Co_3(\mu_3\text{-}CCO_2H)$ in THF gave a homogeneous red-brown solution over period of 12 h. Upon removal of THF, a red-brown microcrystalline solid was isolated in high yield. The microcrystals were soluble in acetone, THF, toluene, and CH_2Cl_2 but insoluble in hexane and diethyl ether. Infrared data indicated that the microcrystals constituted a new compound. Further efforts to recrystallize from $CH_2Cl_2/HOCH_2CH_3$ gave a pure single product, $Ti_6(\mu_3\text{-}O)_4(\mu\text{-}OCH_2CH_3)_4 (OCH_2CH_3)_8\{\mu\text{-}(CO)_9Co_3(\mu_3\text{-}CCO_2)\}_4$, **3**. The solid state infrared spectrum exhibits bands characteristic of the carbonyl groups of the cluster substituent, of bridging carboxylates, and of alkoxide groups. The ^1H and ^{13}C NMR spectra show a single type of ethyl group. As the solid state structure contains two kinds of ethyl groups, the compound must either be fluxional or dissociated in solution. Comparison of the solid state and solution infrared spectra suggests little dissociation in the solvents examined. On the basis of the proposed pathway for **2**, the proposed formation pathway for **3** can be described as follows:

$$4(CO)_9Co_3(\mu_3\text{-}CCO_2H) + 2\{Ti(OCH_2CH_3)_4\}_3 \rightarrow \mathbf{3} + 4C_2H_5OH + 4C_2H_5OC_2H_5$$

$Ti_6(\mu_3\text{-}O)_2(\mu\text{-}O)_2(\mu\text{-}OCH(CH_3)_2)_2(OCH(CH_3)_2)_2(1,2\text{-}O_2C_6H_4)_2)_4\{\mu\text{-}(CO)_9Co_3(\mu_3\text{-}CCO_2)\}_4$, 4. The reaction of $Ti(OCH(CH_3)_2)_4$ with catechol was undertaken first. When $Ti(OCH(CH_3)_2)_4$ was added dropwise to a solution of 2 equiv of catechol in toluene at 50 °C, a red-brown precipitate formed immediately, which was insoluble in a wide variety of solvents. The precipitates were presumably polymeric species and did not react with the cluster acid. Thus, it was determined that the amount of catechol should be reduced to exclude polymerization. $Ti(OCH(CH_3)_2)_4$ was treated with a solution of 1 equiv of catechol in toluene, no precipitate was present, and a homogeneous red solution formed; subsequent addition of $(CO)_9Co_3(\mu_3\text{-}CCO_2H)$ gave a dark red solution over a period of 12 h at 50 °C. Upon removal of all solvent, a black oil was obtained. Fractional crystallization from CH_2Cl_2 gives black crystals in moderate yield. These crystals are soluble in acetone, THF, toluene, and CH_2Cl_2 but insoluble in hexane and diethyl ether. The complicated pattern of bands in the solid state infrared spectra in the region from 900 to 1200 cm^{-1} indicates that there are both isopropoxy and catechol groups. X-ray analysis shows the compound to be a hexamer with the formula $[Ti_6(\mu_3\text{-}O)_2(\mu\text{-}O)_2(\mu\text{-}OCH(CH_3)_2)_2(OCH(CH_3)_2)_2(1,2\text{-}O_2C_6H_4)_4\{\mu\text{-}(CO)_9Co_3\text{-}CCO_2\}_4]$, **4**. The proposed reaction for the formation of compound **4** can be described as follows:

$$Ti(OCH(CH_3)_2)_4 + 1,2\text{-}(OH)_2\text{-}C_6H_4 \rightarrow Ti(OCH(CH_3)_2)_2(1,2\text{-}O_2C_6H_4)$$

$$6Ti(OCH(CH_3)_2)_2(1,2\text{-}O_2C_6H_4) + 4(CO)_9Co_3(\mu_3\text{-}CCO_2H) \rightarrow \mathbf{4} + 2(CH_3)_2CHOCH(CH_3)_2 + 1\text{-}HO\text{-}2\text{-}(CH_3)_2CHO\text{-}C_6H_4 + (CH_3)_2CHOH$$

$[Co_2Ti_2(OCH_2)_3CCH_3)_2(OCH(CH_3)_2)_2\{\mu\text{-}(CO)_9Co_3\text{-}(\mu_3\text{-}CCO_2)\}_4]$, 5. The addition of the polyalcohol $(HOCH_2)_3CCH_3$ to the components that yielded **2a** changes the outcome of the reaction. The core of **5** now contains Co(II) and Ti(IV), and the former can only arise from the degradation of the cluster acid during the synthesis procedure.[41] The solid state infrared spectrum exhibits bands characteristic of the carbonyl group of the cluster substituent, bridging carboxylates, and alkoxide groups, as expected. Because of the complex nature of the cluster degradation, it is not possible to give the reaction equation for the formation of **5**.

$[\{Co_3Ti(OCH_3)_6(HOCH_3)(THF)\{\mu\text{-}(CO)_9Co_3(\mu_3\text{-}CCO_2)\}_3\}_2(O_2CCO_2)]$, 6. The smallest alkoxide, $Ti(OCH_3)_4$, gives an unexpected product which contains Co(II) and an oxalate ligand. Presumably, the latter constitutes one of the organic products accompanying Co(II) formation during the degradation of the tricobalt acid. This degradation appears to be facilitated by CH_3OH.[15] The solid state infrared spectrum exhibits bands characteristic of the carbonyl group of the cluster substituent, bridging carboxylates, and alkoxide groups. However, the carboxylate region is complex and shows an absorption at 1655 cm^{-1}, which is the typical stretching band observed for a tetrabridging oxalate ligand. As with **5**, a reaction for the formation of **6** cannot be given.

Cluster Substituent Effects. The physical properties of the cluster derivatives show some interesting differences from those of their organic analogs. All compounds are colored, and their absorption spectra are qualitatively similar to that of $(CO)_9Co_3(\mu_3\text{-}CCO_2H)$. However, there are perturbations (see Experimental Section), albeit not as dramatic as those observed for $Mo_2\{\mu\text{-}(CO)_9Co_3(\mu_3\text{-}CCO_2)\}_4$.[16,59] The extinction coefficients are roughly proportional to the number of tricobalt units in the cluster assembly. The presence of the carbonyl clusters has a large effect on the intermolecular interactions. For example, compounds **2** with molecular weights of ca. 2500 are soluble in hexane! The compounds all form crystalline, free flowing solids that are not very air sensitive, although they are moisture sensitive.

But it is in the comparison of the reactions of the tricobalt cluster-substituted carboxylic acid and organic acids with group 4 metal alkoxides that important effects associated with the metal cluster are revealed. First, consider the effects on the core structures. These are illustrated in Chart 2 for the compounds containing M(IV) = Ti. Included in the chart are the alkoxide–organic acid combinations that are known to produce the same structure types. Chart 3 shows the effect of

---

(59) Cen, W.; Lindenfeld, P.; Fehlner, T. P. *J. Am. Chem. Soc.* **1992**, *114*, 5451.

Chart 2

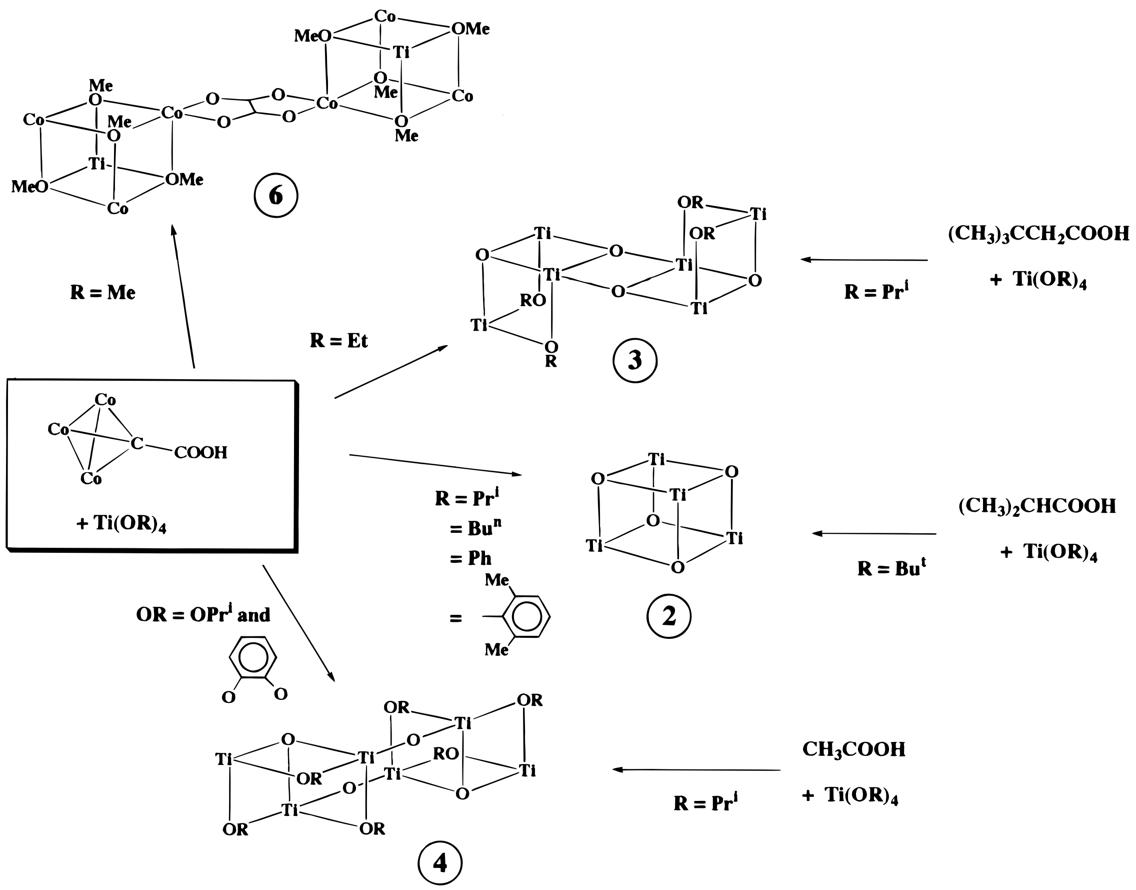

Chart 3

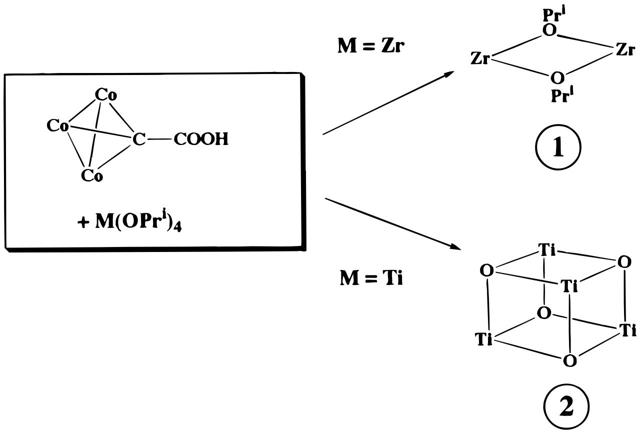

changing metals from Ti(IV) to Zr(IV). Considering the number of possible kinetic and/or thermodynamic effects that might lie behind these differences, it is unrealistic to expect this limited data set to define the differences in any fundamental sense. However, there are a number of points that deserve emphasis.

Perhaps the most striking point is the dominance of structure **2**. For the simple alkoxides, once beyond the ethyl group, large variations in the steric bulk of the organic group does not divert the reaction from the production of structure **2**. The product observed does not depend on the reaction stoichiometry either, i.e., 1:1 and 2:1 (acid to alkoxide) reactant stoichiometries lead to the same the product and the number of cluster carboxylates that coordinate is constant. Contrast this with the behavior of acetic acid. A 1:1 reaction with $Ti(OCHMe_2)_4$ yields a product with four acetates bound to a $Ti_6O_4(OR)_{12}$ framework, whereas a 2:1 reaction yields a product with eight acetates bound to a $Ti_6O_4(OR)_8$ framework.[34]

The number of oxo groups are thought to have an important bearing on the structures observed in related systems. Defining the degree of condensation as y/x for $[Ti_xO_y](OR)_{4x-2y})$, Klemperer et al.[27,60] have suggested that in oxoalkoxides a decrease of the steric repulsion between the organic substituents as the degree of condensation increases might, in general, lead to a significant increase in stability. For **2** $y/x = 1$, whereas for **3** and **4** it is 2/3, but it is doubtful that steric effects alone drive this change. There is a lot of free space in **2a**, for example. On the other hand, the generation of the oxo ligand probably plays a distinct role in the chemistry. On the basis of IR and NMR evidence, the oxo groups in the organic derivatives are often suggested as ultimately arising in the formation of an ester coproduct.[34] In contrast, we have looked for and never observed the stable $(CO)_9Co_3(\mu_3\text{-}CC(O)OR)$ cluster ester as a product but have identified an ether coproduct, ROR, in the formation of the most common compound **2**. Note that ether formation has been shown to accompany oxo ligand formation in related systems.[61,62] It is unlikely that the oxo groups are generated from a trace amount of water in the crystalline cluster acid, although water is removed from the cluster acid only

---

(60) Campana, C. F.; Chen, Y.; Day, V. W.; Klemperer, W. G.; Sparks, R. A. *J. Chem. Soc., Dalton Trans.* **1996**, 691.

(61) Turova, N. Y.; Kessler, V. G.; Kucheiko, S. I. *Polyhedron* **1991**, *10*, 2617.

(62) Sirio, C.; Hubert-Pfalzgraf, L. G.; Bois, C. *Polyhedron* **1997**, *16*, 1129.

with difficulty. Deliberate addition of stoichiometric amounts of H_2O at various points in the reaction procedure leads to totally different chemistry plus decomposition of the cluster ligands. Further, identical cluster acid samples lead to **1** and **6**, neither of which contain an oxo group.

In contrast to the organic acids where the number of acids incorporated can be varied to some extent, all of these compounds except **6** contain four cluster carboxylates. This is clearly not due to steric effects in the final product. First, the cubane-like structures of **2** are formed in spite of large changes in the steric requirements of the organic substituent on the alkoxide ligand. Only with the ethoxide ligand and the bidentate alkoxide are different core structures observed. Second, steric factors do not limit the number of clusters associated with a given core as with different synthetic strategies in which compounds with three, five, and six cluster carboxylates coordinated have been observed.[13,41,63] In each of these cases, the cationic metal core is arguably similar in size to the $[Ti_4O_4]^{8+}$ cubane cores of **2** and smaller than those of **3**, **4**, and **6**.

One possible explanation for the limited number of cobalt clusters incorporated is that the products are generated from smaller units that contain a fixed number of firmly bound cluster carboxylates. For **2**, we suggest the active species is $Ti(OR)_3\{(CO)_9Co_3(\mu_3\text{-}CCO_2)\}$. This hypothesis is consistent with the observed rapid reaction of $(CO)_9Co_3(\mu_3\text{-}CCO_2H)$ with $Ti(OR)_4$, and formation of **2** would simply require the rate of condensation to be more rapid than addition of another cluster ligand. The fact that the oligomeric nature of the alkoxide in solution depends on the size of the R group, i.e., for $R = C_2H_5$, the alkoxide is trimeric in solution whereas for $R = CH(CH_3)_2$ it is monomeric,[54,64] can be used to explain the different behavior of the ethoxide. Here, we suggest that the rate of addition of a third large cluster ligand is slow relative to $Ti_3(OCH_2CH_3)_{10}\{(CO)_9Co_3(\mu_3\text{-}CC(O)O)\}_2$ dimerization to yield **3**. If we assume that the reaction of catechol with $Ti(OCH(CH_3)_2)_4$ yields a trimer, then $Ti_3(OCH(CH_3)_2)_6(1,2\text{-}O_2C_6H_4)_2\{(CO)_9Co_3(\mu_3\text{-}CC(O)O)\}_2$ is an appealing precursor for **4** simply because a terminal/bridging catechol trimer with two cluster ligands could not undergo the edge-to-edge coupling that results in **3** (Chart 2).

All these differences point to a larger role of electronic effects in the reaction chemistry for the inorganic cluster carboxylate vs the organic carboxylates. That is, the cluster substituent appears to introduce a higher degree of chemical discrimination either in the kinetics of formation or in the product stability. Thus, for the protonolysis of a metal alkoxide with a cluster acid, the product wells must either have sufficiently different energies or sufficiently different energy barriers such that the free energy associated with concentration changes has little effect on the product identity and steric effects generated by the alkoxide and the cluster acid are not important as they are for organic acids. This electronic effect is reflected in the lower acidity of the cluster acid relative to an organic acid and suggests greater ligand binding of the cluster carboxylate relative to an organic carboxylate.

The M(IV) metal also plays a role in the chemistry, as emphasized by Chart 3. In this case, protonolysis of four of the alkoxide ligands of the dimeric Zr(IV) starting material takes place, but no further condensation occurs. In contrast to Ti(IV), the larger Zr(IV) permits seven coordination and the ready addition of two cobalt cluster ligands per Zr center. Compound **1** might be considered a model for a dimeric intermediate in the formation of **2**, which has been trapped by the addition of two more cobalt cluster ligands. Thus, dimerization of the hypothetical $Ti_2(\mu\text{-}OR)_2(OR)_4\{\mu\text{-}(CO)_9Co_3(\mu_3\text{-}CCO_2)\}_2$ intermediate by elimination of four ROR molecules is a formal route to the dominant product type.

Finally, an aspect of the cluster acid that distinguishes it from organic acids is that slow degradation of the tricobalt cluster produces Co(II) ions (and other fragments, e.g., oxalate ions) that can get involved in the reaction chemistry. Aggressive or long reaction times inevitably lead to the formation of $[Co_2\{(CO)_9Co_3(\mu_3\text{-}CCO_2)\}_4]$,[15] but intermediate conditions sometimes result in the isolation of mixed-metal MCo(II) compounds, i.e., **5** and **6** in this instance. In all cases, modest to good yields of a single cluster derivative are obtained despite the lack of any external control over Co(II) stoichiometry. The observation of a single reaction pathway producing good yields corroborates the above suggestion that the cluster substituent increases the chemical selectivity of the carboxylate moiety.

Acknowledgment. We thank Prof. W. G. Klemperer and Dr. Timothy J. Boyle for comments and information in advance of publication, and we are grateful for the support of the National Science Foundation and a Reilly Fellowship of the Department of Chemistry and Biochemistry held by X.L.

Supporting Information Available: Text giving an intercomparison of the structural metrics of compounds **1**−**6** and tables of crystal data, positional and equivalent isotropic thermal parameters, bond distances and angles, and general displacement parameter expressions and ORTEP drawings for **1**, **2b**, **2d**, **5**, and **6** (136 pages). Ordering information is given on any current masthead page. The crystal data and related metrics data for **2a**, **2c**, **3**, and **4** have been deposited elsewhere.[35]

OM970837B

---

(63) Calvo-Perez, V. Ph.D. Thesis, University of Notre Dame, Notre Dame, IN, 1995.

(64) Babonneau, F.; Doeuff, S.; Leaustic, A.; Sanchez, C.; Cartier, C.; Verdaguer, M. *Inorg. Chem.* **1988**, *27*, 3166.